

# Assessing Per-Sample Membership Inference Vulnerability without Retraining

Valentin Dorseuil \*  
DI ENS, École normale supérieure  
Université PSL, CNRS

Jamal Atif  
CMAP, École polytechnique  
Institut Polytechnique de Paris

Olivier Cappé  
DI ENS, École normale supérieure  
Université PSL, CNRS

## Abstract

Recent work in the privacy literature shows that sample-targeted membership inference attacks (MIAs) significantly outperform untargeted approaches by a wide margin. Motivated by this observation, we address the following question: *can the privacy vulnerability of individual training points be assessed without training shadow models?* We show that per-sample exposure to MIA is governed not only by a point's loss, but also by a data-dependent geometric measure. In the linear setting, we derive a closed-form decomposition of individual black-box MIA vulnerability into a population leverage score and a residual loss term, making explicit how sample-dependent geometry translates into privacy exposure. Since the final layer of most modern architectures is linear, we extend this framework to deep networks and propose a surrogate score operating on last-layer representations that requires only a single trained model and no shadow models. Empirical evaluations across diverse datasets and architectures show that our score outperforms loss and gradient-norm baselines at identifying the highest-risk points under state-of-the-art attacks, providing a computationally efficient and theoretically grounded tool for per-sample privacy risk assessment.

## 1 Introduction

Modern machine learning models, and deep neural networks in particular, are known to memorize aspects of their training data [Zhang et al., 2017, Carlini et al., 2019]. This memorization induces privacy vulnerabilities that can be exploited by *Membership Inference Attacks* (MIAs), which aim to determine whether a specific data point was included in the training set or not [Shokri et al., 2017, Carlini et al., 2022a]. A principled defense against membership inference is provided by Differential Privacy (DP) [Dwork, 2006], implemented in deep learning through noise injection in stochastic gradient methods [Abadi et al., 2016]. However, controlling the trade-off between privacy protection and model utility remains challenging. Noise calibration typically relies on worst-case theoretical accounting, paired with empirical privacy auditing via MIAs, and often leads to either overly conservative noise levels or insufficient privacy protection. In this context, designing MIAs for empirical auditing is essential to quantify privacy leakage in non-privately trained models [Yeom et al., 2018] or to validate the practical tightness of DP guarantees in privately trained models [Nasr et al., 2021, Jagielski et al., 2020].

---

\*Corresponding author: [valentin.dorseuil@ens.psl.eu](mailto:valentin.dorseuil@ens.psl.eu)  
Preprint under review.

While such auditing is now standard practice [Carlini et al., 2022a, Nasr et al., 2021, Zarifzadeh et al., 2024], relying on aggregate metrics such as average accuracy or AUC is insufficient. These global measures can obscure critical risk heterogeneity, as outliers and rare subgroups are significantly more prone to memorization than typical samples [Carlini et al., 2022a, Feldman and Zhang, 2020]. Consequently, a model certified as private on average may still expose specific points to high privacy risks. To address this heterogeneity, recent work is increasingly focusing on *per-sample* privacy risk assessment, aiming to quantify membership leakage at the level of each data point, separately, rather than in aggregate. State-of-the-art methods for per-sample auditing [Carlini et al., 2022a, Zarifzadeh et al., 2024] predominantly rely on *shadow models*. These techniques train multiple shadow models on random data splits to characterize each data point’s influence on the model’s behavior. This enables identification of which points exhibit increased sensitivity to their presence in the training dataset. However, these techniques are computationally prohibitive, especially for large-scale models, as they require retraining the model many times. This leads to our central question stated in the abstract: *can the privacy vulnerability of individual training points be assessed without training shadow models?*

To address this question in a principled way, we first consider the baseline case of Gaussian linear regression. Even in this simple model, the task poses interesting challenges: the fixed-design analysis from classical statistics leads to the *leverage score* (see below), which quantifies a data point’s geometric influence solely through its feature vector, ignoring the response. The fully randomized approach, on the other hand, provides metrics that depend on general problem characteristics (dimensions, covariance operator of the features) but do not account for specific data points (see, e.g., Tan et al. [2022]). To obtain relevant per-sample risk exposure metrics, we propose to consider non-asymptotic results in the randomized Gaussian setting by *conditioning on a single data point* (i.e., its feature vector and its response).

For Gaussian linear regression, we derive a closed-form expression for the expected leave-one-out generalization gap, the signal exploited by state-of-the-art black-box attacks such as LiRA [Carlini et al., 2022a], and show that it decomposes, at first order, into a response-free geometric term, the population leverage score  $\bar{h}_{ii}$ , and a response-dependent structural error  $\varepsilon_i$ . Membership inference vulnerability is therefore governed jointly by a point’s geometric measure and its structural error. Samples that are both geometrically influential in shaping the model’s parameters and poorly fit by the model are at the highest risk of privacy leakage.

To extend this analysis beyond the linear setting, we approximate the leave-one-out loss gap using two classical estimators: an influence-function estimate and a Newton-step estimate. Restricted to the last layer of a trained network, both admit closed-form expressions in terms of the leverage score of the learned representations, and can be computed from a single trained model at negligible cost. This yields a scalable, theoretically grounded proxy for per-sample privacy risk that tracks the rankings produced by state-of-the-art shadow-model attacks, without any retraining.

The paper is organized as follows. In Section 3 we derive a closed-form expression for the expected leave-one-out generalization gap of a target point in Gaussian linear regression, showing that the signal driving LiRA-style attacks decomposes, at first order, into a label-free geometric term, the population leverage  $\bar{h}_{ii}$ , and a label-dependent structural error  $\varepsilon_i$ . In Section 4, we propose two retraining-free per-sample vulnerability scores for general differentiable models, based, respectively, on influence-function and Newton-step approximations of the leave-one-out loss. Restricted to the last layer, both admit closed-form expressions in terms of the leverage score of the last-layer representation, which can be efficiently computed for deep networks. Finally, Section 5 reports the performance of the proposed vulnerability scores in terms of recovery of the results obtained by state-of-the-art retraining-based MIA methods. In particular, we observe that the proposed metrics consistently outperform commonly used

baselines, such as training loss or terminal gradient-norm, across various configurations of dataset/architecture pairs. We start with a quick review of the relevant literature.

## 2 Related Work

**Membership Inference Attacks.** Membership inference aims to determine if a specific sample was used to train a model. Early approaches relied on simple metric-based classifiers, exploiting overfitting signals such as prediction confidence, entropy, or the magnitude of gradients [Shokri et al., 2017, Yeom et al., 2018]. While computationally inexpensive, these methods often struggle to distinguish between a "vulnerable" member and a "hard" non-member.

To address this, current state-of-the-art methods adopt the *shadow model* paradigm [Shokri et al., 2017]. By training multiple models on different data splits, attacks like LiRA (Likelihood Ratio Attack) [Carlini et al., 2022a] or RMIA (Robust Membership Inference Attack) [Zarifzadeh et al., 2024] essentially perform a hypothesis test on the loss distribution of a target point [Zarifzadeh et al., 2024]. While highly effective, these approaches are computationally prohibitive, often requiring hundreds of training runs to estimate the risk for a single point accurately. Our work seeks to achieve the precision of these hypothesis-test based methods without their computational burden, by substituting retraining with geometric analysis.

**Influence Functions and Data Attribution.** Recent work has begun to explore the connection between influence and privacy. Notably, Feldman and Zhang [2020] and Feldman [2020] link the *memorization* of a sample to its influence on the learning process, arguing that memorization is necessary for generalization in long-tailed distributions. Other work has used influence functions to craft new attack methods [Cohen and Giryes, 2024, Suri et al., 2024], but these approaches inherit two well-known limitations of influence functions in deep learning: a prohibitive computational cost, and a fragility that often renders the resulting estimates unreliable [Basu et al., 2021].

Our work addresses these limitations by confining influence estimation to the last layer, where closed-form expressions are available. This reduces the computational overhead and avoids the fragility of full-network influence, while remaining a faithful proxy of per-sample influence as shown in our experiments.

**Privacy Auditing and Heterogeneity.** Differential Privacy (DP) [Dwork, 2006] provides worst-case guarantees for membership privacy. Using algorithms such as DP-SGD [Abadi et al., 2016], one can train Deep Learning models to be private. However, these bounds are often loose and do not capture the empirical reality that privacy risk is non-uniform: some outlier samples are far more exposed than others [Zarifzadeh et al., 2024].

Auditing per-sample privacy risk, i.e., estimating the specific  $(\epsilon, \delta)$  DP parameters for a given sample, remains an open challenge. Existing auditing tools rely heavily on the aforementioned shadow model techniques or randomized smoothing [Lecuyer et al., 2019], which scale poorly. Our work contributes to this domain by proposing an efficient individual privacy-risk metric for identifying vulnerable samples. This approach complements existing auditing frameworks by providing a first-pass, zero-retraining filter for high-risk data points. Removing these vulnerable points from the training set is not an option since, in practice, such deletions often expose new points, an effect described as the *privacy onion effect* by Carlini et al. [2022b]. Instead, our method can serve as a tool for canary selection [Carlini et al., 2019] or per-sample privacy training [Wang, 2018, Alaggan et al., 2017].

### 3 Analysis of Membership Vulnerability in the Linear Regression Case

To rigorously understand the privacy leakage exploited by black-box attacks, we first analyze their behavior within the context of linear models. State-of-the-art MIAs, such as shadow model classifiers [Shokri et al., 2017], LiRA [Carlini et al., 2022a], and RMIA [Zarifzadeh et al., 2024], compute membership scores via classifiers or likelihood ratio tests fitted to per-sample losses. In practice, they estimate the loss distribution of each sample, conditioned on whether it was included in the training set, by training shadow models on multiple data splits.

To model the stochasticity of training on random subsamples, we isolate a fixed target point  $i$  and treat the remainder of the dataset as being drawn from an underlying probability distribution. We then analyze the marginal distribution of the target’s loss under two scenarios: the IN setting, where the model is trained on the fixed point alongside the samples drawn from the distribution, and the OUT setting, where the model is trained exclusively on the sampled distribution without the target point.

#### 3.1 Problem Setup and Notation

Let  $\mathcal{Z} \subset \mathbb{R}^p \times \mathbb{R}$  be the data space, and let  $z_i = (x_i, y_i) \in \mathcal{Z}$  be a fixed target observation. Throughout our analysis, we condition on this target point, treating it as a deterministic constant. We consider a full training dataset  $S$  of size  $n$  that contains this fixed target  $z_i$ . The other  $n - 1$  points in  $S$ , denoted collectively as  $S_{-i} = \{(X_j, Y_j)\}_{j \neq i}$ , are random variables sampled from the underlying data distribution.

Because  $z_i$  is fixed, the randomness in our estimators arises entirely from these  $n - 1$  background observations. We assume their covariates are drawn i.i.d. from a multivariate Gaussian distribution,  $X_j \sim \mathcal{N}(0, \Sigma)$ , and their responses follow the linear generative model  $Y_j | X_j \sim \mathcal{N}(X_j^\top \theta, \sigma^2)$  where  $\theta \in \mathbb{R}^p$  is the unknown true parameter and  $\sigma^2$  the structural noise variance. We consider the scalar response case for simplicity, and the results are extended to multivariate responses in Appendix A.

Let  $X \in \mathbb{R}^{n \times p}$  denote the full design matrix, where the  $i$ -th row is the deterministic  $x_i^\top$  and the remaining rows form the random submatrix  $X_{-i} \in \mathbb{R}^{(n-1) \times p}$ . Similarly, let  $Y \in \mathbb{R}^n$  be the response vector containing  $y_i$  and the random subvector  $Y_{-i} \in \mathbb{R}^{n-1}$ .

Let  $\hat{\theta} = (X^\top X)^{-1} X^\top Y$  be the ordinary least squares (OLS) estimator trained on the full dataset  $S$ , and  $\hat{\theta}_{-i}$  be the estimator trained on  $S_{-i}$ . We denote  $e_i = y_i - x_i^\top \hat{\theta}$  the residual for the target point under the full model and  $e_{-i} = y_i - x_i^\top \hat{\theta}_{-i}$  the residual for the target point under the leave-one-out model. The corresponding squared residuals are the training loss  $\ell_i = (y_i - x_i^\top \hat{\theta})^2$  and the leave-one-out loss  $\ell_{-i} = (y_i - x_i^\top \hat{\theta}_{-i})^2$ .

We introduce the leverage matrix  $H = X(X^\top X)^{-1} X^\top$ , and denote  $h_{ii} = x_i^\top (X^\top X)^{-1} x_i$  the empirical leverage score of the target point, which is the  $i$ -th diagonal element of  $H$ . This score is a random variable due to its dependence on  $X_{-i}$ , and quantifies the geometric influence of the point on its own fitted value [Belsley et al., 1980] illustrated by the leave-one-out identity  $e_i = (1 - h_{ii}) e_{-i}$  [Allen, 1974].

We define two deterministic quantities characterizing the target point: its population leverage score  $\bar{h}_{ii} = x_i^\top \Sigma^{-1} x_i$ , which corresponds to the squared Mahalanobis distance to the feature distribution, and its structural error  $\varepsilon_i = y_i - x_i^\top \theta$ .

Our goal is to characterize the distribution of the losses  $\ell_i$  and  $\ell_{-i}$  and see how these distributions relate to the target point’s MIA vulnerability.

### 3.2 Finite-Sample Distributions of Leverage Score and Loss

We begin by analyzing the leave-one-out Gram matrix  $G_{-i} = X_{-i}^\top X_{-i}$ , which follows a Wishart distribution  $\mathcal{W}_p(\Sigma, n-1)$  [Muirhead, 1982]. Applying the Sherman–Morrison–Woodbury identity allows us to express both the empirical leverage score  $h_{ii}$  and the leave-one-out residual  $e_{-i}$  as functions of  $G_{-i}$ , thereby isolating the geometric randomness of the design from the structural noise. The following lemma makes this decomposition explicit.

**Lemma 3.1** (Joint Law of Leverage Scores and Residuals). *Let  $G_{-i} = X_{-i}^\top X_{-i}$  denote the leave-one-out Gram matrix, which follows a Wishart distribution  $\mathcal{W}_p(\Sigma, n-1)$  [Muirhead, 1982]. We define*

$$V = \frac{\bar{h}_{ii}}{x_i^\top G_{-i}^{-1} x_i}, \quad Z = -\frac{\sqrt{V}}{\sigma \sqrt{\bar{h}_{ii}}} x_i^\top G_{-i}^{-1} X_{-i}^\top \varepsilon_{-i}. \quad (1)$$

Then, the empirical leverage score  $h_{ii}$  and the leave-one-out residual  $e_{-i}$  satisfy the identities:

$$h_{ii} = \frac{\bar{h}_{ii}}{V + \bar{h}_{ii}}, \quad e_{-i} = \varepsilon_i + \sigma \frac{\sqrt{\bar{h}_{ii}}}{\sqrt{V}} Z. \quad (2)$$

Moreover, conditioned on  $(x_i, y_i)$ ,  $V \sim \chi_{n-p}^2$  and  $Z \sim \mathcal{N}(0, 1)$ , with  $Z \perp\!\!\!\perp V$ .

The independence of  $Z$  and  $V$  in Lemma 3.1 is an important property: given  $X_{-i}$ , the standardized prediction error  $Z$  is  $\mathcal{N}(0, 1)$  regardless of the design, hence independent of any function of it, including  $V$ . Combining the leave-one-out identity  $e_i = (1 - h_{ii})e_{-i}$  [Allen, 1974], which gives  $\ell_i = (1 - h_{ii})^2 \ell_{-i}$ , with Lemma 3.1, we obtain a full characterization of the joint distribution of the losses at point  $i$  in Proposition 3.2.

**Proposition 3.2** (Per-sample Loss Distribution). *Under the Gaussian linear regression model, the leave-one-out loss  $\ell_{-i}$  and the training loss  $\ell_i$  at a point  $(x_i, y_i)$  satisfy*

$$\ell_{-i} = \left( \varepsilon_i + \sigma \frac{\sqrt{\bar{h}_{ii}}}{\sqrt{V}} Z \right)^2, \quad \ell_i = \left( \varepsilon_i + \sigma \frac{\sqrt{\bar{h}_{ii}}}{\sqrt{V}} Z \right)^2 \left( \frac{V}{V + \bar{h}_{ii}} \right)^2, \quad (3)$$

where  $V$  and  $Z$  are defined in Lemma 3.1, satisfying  $V \sim \chi_{n-p}^2$  and  $Z \sim \mathcal{N}(0, 1)$ , with  $Z \perp\!\!\!\perp V$ .

### 3.3 Per-Point Vulnerability under Optimal Inference

Using Proposition 3.2 and the Neyman–Pearson Lemma [Neyman and Pearson, 1933], we derive the optimal black-box attack in closed form. In the large-sample regime  $n - p \gg 1$ , the variable  $V \sim \chi_{n-p}^2$  concentrates sharply around its mean, so we replace it by the constant  $n - p$  and Proposition 3.2 reduces to a deterministic rescaling in distribution:  $\ell_i | \mathcal{H}_{\text{IN}} = c_i^2 \cdot (\ell_{-i} | \mathcal{H}_{\text{OUT}})$ , with the scale factor  $c_i^2 = ((n - p)/(n - p + \bar{h}_{ii}))^2 < 1$ . The likelihood ratio is then monotone in the observed loss, so the Neyman–Pearson optimal test thresholds  $\ell_{i, \text{obs}}$  directly.

**Corollary 3.3** (Optimal MIA Trade-off). *Let  $F_{i, \text{OUT}}$  denote the CDF of  $\ell_{-i}$  under  $\mathcal{H}_{\text{OUT}}$ . For any target false positive rate  $\alpha_i \in (0, 1)$ , the false negative rate of the Neyman–Pearson optimal attack at point  $i$  is*

$$\beta_i(\alpha_i) = 1 - F_{i, \text{OUT}}\left(\frac{1}{c_i^2} F_{i, \text{OUT}}^{-1}(\alpha_i)\right). \quad (4)$$

The closed-form expression itself follows from a standard Neyman–Pearson argument; the corollary’s value lies in clarifying *which* features of the problem dictate vulnerability. The full trade-off function  $\alpha_i \mapsto \beta_i(\alpha_i)$  depends on the data only through  $(\bar{h}_{ii}, \varepsilon_i)$  and the global parameters  $(n, p, \sigma^2)$ . In particular, the entire design matrix  $X_{-i}$  enters only through the scalar population leverage  $\bar{h}_{ii}$ . The pair  $(\bar{h}_{ii}, \varepsilon_i)$  thus acts as a per-point sufficient statistic for membership-inference vulnerability.

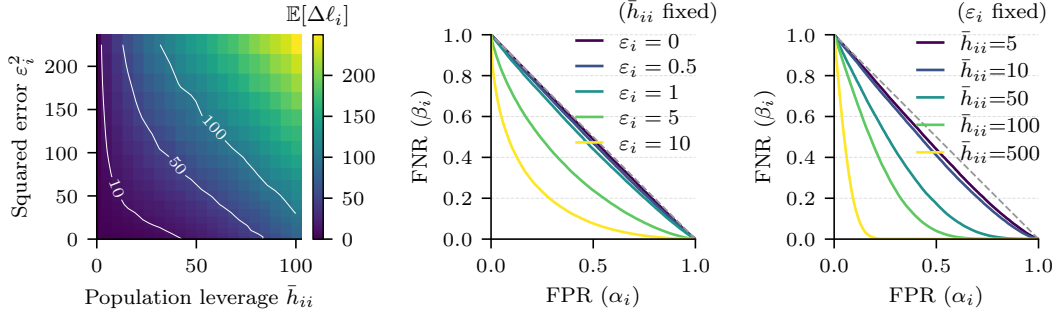


Figure 1: Generalization gap and membership inference attack performance for the Gaussian linear regression model. **(left)** Heatmap of the generalization gap  $\mathbb{E}[\Delta\ell_i]$  as a function of  $\varepsilon_i^2$  and  $\bar{h}_{ii}$ , estimated with Monte-Carlo. **(middle)** Theoretical false negative rate (FNR)  $\beta_i$  of the optimal attack on the point  $i$  as a function of the false positive rate (FPR)  $\alpha_i$ , for different values of the structural error  $\varepsilon_i$ , with  $\bar{h}_{ii} = 1$  and  $\sigma^2 = 1$ . **(right)** Same as (middle) but with fixed  $\varepsilon_i = 1$  and  $\bar{h}_{ii}$  varying.

### 3.4 The Expected Generalization Gap

Alongside the trade-off curve, the expected generalization gap  $\mathbb{E}[\Delta\ell_i]$  has been identified as the fundamental theoretical bound on the power of loss-based MIAs [Yeom et al., 2018]. In our model, it admits a theoretical closed-form and a tractable asymptotic expression that make the dependence on  $(\bar{h}_{ii}, \varepsilon_i)$  explicit.

**Proposition 3.4** (Expected Generalization Gap). *For  $n - p > 2$ , the expected difference between the leave-one-out and training loss for a fixed point  $(x_i, y_i)$  is exactly:*

$$\mathbb{E}[\Delta\ell_i] = \mathbb{E}_{V \sim \chi_{n-p}^2} \left[ \left( \varepsilon_i^2 + \sigma^2 \frac{\bar{h}_{ii}}{V} \right) \frac{\bar{h}_{ii}(2V + \bar{h}_{ii})}{(V + \bar{h}_{ii})^2} \right]. \quad (5)$$

The asymptotic expansion of this gap in powers of  $(n - p)^{-1}$  is:

$$\mathbb{E}[\Delta\ell_i] = \frac{2\varepsilon_i^2 \bar{h}_{ii}}{n - p} + \frac{4\varepsilon_i^2 \bar{h}_{ii} + \bar{h}_{ii}^2(2\sigma^2 - 3\varepsilon_i^2)}{(n - p)^2} + \mathcal{O}\left(\frac{1}{(n - p)^3}\right). \quad (6)$$

Proposition 3.4 establishes that, to first order, the generalization gap is governed by the interaction between a point’s structural error  $\varepsilon_i^2$  and its leverage  $\bar{h}_{ii}$ . Intuitively, the points exhibiting the largest generalization gap are those that are simultaneously outliers in feature space (high  $\bar{h}_{ii}$ ) and difficult to predict (high  $\varepsilon_i^2$ ). Moreover, the gap vanishes at a rate of  $1/n$ , which confirms that the privacy risk associated with any individual point diminishes as the size of the dataset grows.

Figure 1 illustrates Corollary 3.3 and Proposition 3.4 using Monte-Carlo simulations. The left panel shows how the expected generalization gap grows with the true residual  $\varepsilon_i^2$  and the leverage score  $\bar{h}_{ii}$ . The middle and right panels present the trade-off curves of the optimal MIA for varying  $\bar{h}_{ii}$  and  $\varepsilon_i^2$ , respectively, confirming that the attack’s statistical power increases monotonically in both parameters.

Proofs for all the results presented in this section are deferred to Appendix A.

## 4 Generalization to Non-Linear Models

In the linear regression case, we could derive the exact value of the loss gap  $\ell_{-i} - \ell_i$  without retraining. This is because the OLS estimator has a closed-form solution and the loss

is quadratic. For more general models, such as generalized linear models or deep neural networks, we do not have closed-form solutions. In the following, we discuss how common techniques from influence functions and Newton steps can be used to estimate the loss gap without retraining, and how they relate to the previous analysis in both the linear regression and the logistic regression case.

## 4.1 Influence Functions and Newton Step

**Influence Function.** Influence functions [Hampel, 1974, Koh and Liang, 2017] provide a way to estimate the effect of removing a training point  $z_i$  on the model parameters  $\hat{\theta}$  without retraining. Formally, the influence of  $z_i$  is defined as:

$$I(z_i) = -\left[\frac{1}{n} \sum_{j=1}^n \nabla_{\theta}^2 \ell(\hat{\theta}, z_j)\right]^{-1} \nabla_{\theta} \ell(\hat{\theta}, z_i).$$

Using a first-order Taylor expansion, this defines our first estimator for the loss gap, which we call the *Influence Function estimator*:

$$\widehat{\Delta \ell}_i^{\text{IF}} = \nabla_{\theta} \ell(\hat{\theta}, z_i)^{\top} \left[ \sum_{j=1}^n \nabla_{\theta}^2 \ell(\hat{\theta}, z_j) \right]^{-1} \nabla_{\theta} \ell(\hat{\theta}, z_i). \quad (7)$$

**Newton Step.** Alternatively, one can approximate the loss gap by taking a single Newton step on the leave-one-out objective starting from  $\hat{\theta}$ . Using a first-order Taylor expansion on the loss, this defines our second estimator, which we call the *Newton Step estimator*:

$$\widehat{\Delta \ell}_i^{\text{NS}} = -\nabla_{\theta} \ell(\hat{\theta}, z_i)^{\top} \left[ \frac{1}{n} \sum_{j \neq i} \nabla_{\theta}^2 \ell(\hat{\theta}, z_j) \right]^{-1} \frac{1}{n} \sum_{j \neq i} \nabla_{\theta} \ell(\hat{\theta}, z_j).$$

Notably, when the model has fully converged and minimizes the empirical risk (i.e.,  $\frac{1}{n} \sum_{j=1}^n \nabla_{\theta} \ell(\hat{\theta}, z_j) = 0$ ), it follows that  $\frac{1}{n} \sum_{j \neq i} \nabla_{\theta} \ell(\hat{\theta}, z_j) = -\frac{1}{n} \nabla_{\theta} \ell(\hat{\theta}, z_i)$ . Under this convergence assumption, the Newton Step estimator simplifies to:

$$\widehat{\Delta \ell}_i^{\text{NS}} = \nabla_{\theta} \ell(\hat{\theta}, z_i)^{\top} \left[ \sum_{j \neq i} \nabla_{\theta}^2 \ell(\hat{\theta}, z_j) \right]^{-1} \nabla_{\theta} \ell(\hat{\theta}, z_i), \quad (8)$$

a form also known as the *Approximate Leave-One-Out* (ALO) estimator in the statistics literature and used in approximate unlearning methods [Guo et al., 2020, Sekhari et al., 2021].

Remarkably,  $\widehat{\Delta \ell}_i^{\text{IF}}$  and  $\widehat{\Delta \ell}_i^{\text{NS}}$  coincide up to a rank-one correction of the Hessian, despite being derived from distinct principles. In the following section, we derive closed-form expressions for these two estimators in the context of linear and logistic regression, and show how they can serve as scalable proxies for the loss gap to evaluate vulnerability to membership inference attacks.

## 4.2 Analysis for Linear Regression and Logistic Regression

We now derive the exact expressions of  $\widehat{\Delta \ell}_i^{\text{IF}}$  and  $\widehat{\Delta \ell}_i^{\text{NS}}$  for linear and logistic regression. These are not further approximations: they are the direct, closed-form instantiations of Equations (7) and (8) for the respective model classes.

**Linear Regression.** In linear regression, the OLS estimator  $\hat{\theta} = (X^\top X)^{-1}X^\top Y$  is available in closed form and the loss is quadratic, so both estimators admit exact closed-form expressions. Letting  $e_i$  denote the residual and  $h_{ii}$  the leverage score, the two estimators yield:

$$\widehat{\Delta\ell}_i^{\text{IF}} = 2e_i^2 h_{ii}, \quad \widehat{\Delta\ell}_i^{\text{NS}} = \frac{2e_i^2 h_{ii}}{1 - h_{ii}}. \quad (9)$$

The Newton Step estimator introduces a leverage correction  $(1 - h_{ii})^{-1}$ , bringing it closer to the exact leave-one-out formula:  $\Delta\ell_i = e_i^2(2h_{ii} - h_{ii}^2)/(1 - h_{ii})^2$ , particularly for high-leverage points.

**Logistic Regression.** In binary logistic regression, with  $\hat{p}_i = \sigma(\hat{\theta}^\top x_i)$ , the two estimators yield:

$$\widehat{\Delta\ell}_i^{\text{IF}} = \frac{(y_i - \hat{p}_i)^2}{w_i} h_{ii}, \quad \widehat{\Delta\ell}_i^{\text{NS}} = \frac{(y_i - \hat{p}_i)^2}{w_i} \frac{h_{ii}}{1 - h_{ii}}, \quad (10)$$

where  $w_i = \hat{p}_i(1 - \hat{p}_i)$  and  $h_{ii} = w_i x_i^\top (X^\top W X)^{-1} x_i$  is the weighted leverage score, with  $W = \text{diag}(w_j)_{j=1, \dots, n}$ . This is the logistic regression analogue of the OLS leverage score [Pregibon, 1981]: in both cases,  $h_{ii}$  captures the local sensitivity of the fitted response to the target,  $\partial\hat{y}_i/\partial y_i$  in linear regression and  $\partial\hat{p}_i/\partial y_i$  in logistic regression. As in Equation (9), the Newton Step estimator applies a leverage correction relative to the Influence Function estimator.

We generalize both of these results for the multivariate case in Appendix B.6. Motivated by these findings, as well as our theoretical analysis in Proposition 3.4, we propose to use these estimates as proxies for vulnerability assessment in deep neural networks. In practice, we consider only the linear last layer of the network, and apply the estimators defined in equations (9) and (10) (or their multivariate counterparts) depending on the loss used for the training (cross-entropy for classification, quadratic for regression).

### 4.3 Differences Between the two Approaches

In both linear and logistic regression, the two estimators differ by a single multiplicative factor:  $\widehat{\Delta\ell}_i^{\text{NS}}/\widehat{\Delta\ell}_i^{\text{IF}} = 1/(1 - h_{ii})$ . At low leverage they therefore agree to leading order. The correction matters only as  $h_{ii} \rightarrow 1$ , a regime reached, for instance, when  $x_i$  is orthogonal to every other row of  $X$ , in which case  $h_{ii} = 1$  exactly. We have:

$$\frac{\widehat{\Delta\ell}_i^{\text{IF}}}{\Delta\ell_i} \underset{h_{ii} \rightarrow 1}{\sim} 2(1 - h_{ii})^2, \quad \frac{\widehat{\Delta\ell}_i^{\text{NS}}}{\Delta\ell_i} \underset{h_{ii} \rightarrow 1}{\sim} 2(1 - h_{ii}).$$

As  $h_{ii} \rightarrow 1$ , both estimators vanish relative to  $\Delta\ell_i$ , but at different rates: the Influence Function estimator captures only an  $O((1 - h_{ii})^2)$  fraction of the true loss change, whereas the Newton Step estimator captures an  $O(1 - h_{ii})$  fraction. The Newton Step therefore tracks the per-sample generalization gap substantially better than the Influence Function at high-leverage points.

Proofs for all the results presented in this section are deferred to Appendix B.

## 5 Experiments

### 5.1 Experimental Setup

We evaluate our two surrogates  $\widehat{\Delta\ell}_i^{\text{IF}}$  and  $\widehat{\Delta\ell}_i^{\text{NS}}$  for per-sample membership-inference vulnerability across a diverse set of modalities, architectures and learning regimes.

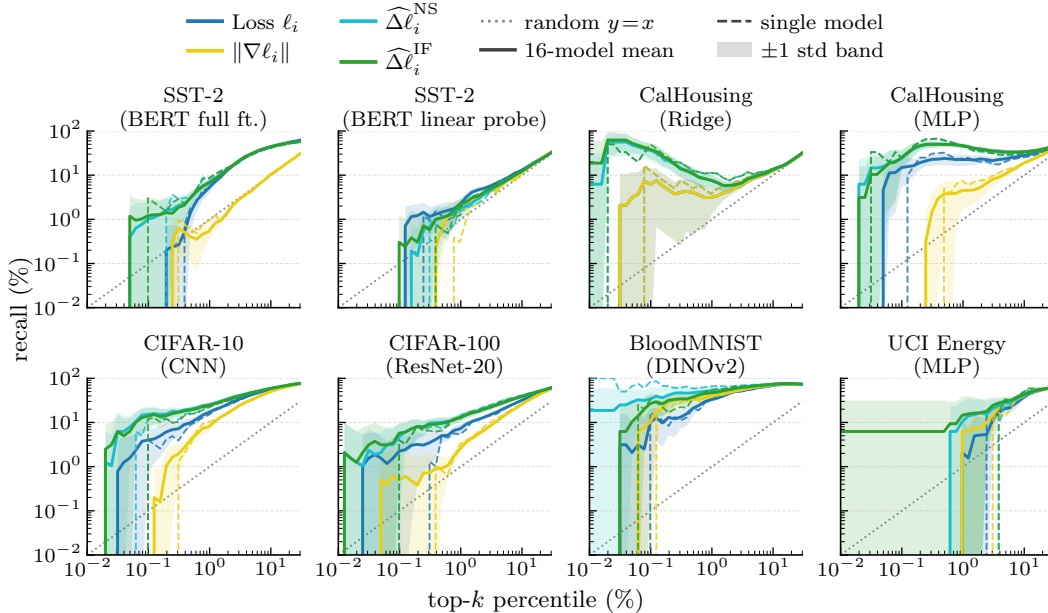


Figure 2: Recall of the top- $k$ % LiRA’s attack most vulnerable samples (ranked by the Average Success Rate) when keeping the top- $k$ % for each of the four surrogate: the loss  $\ell_i$ , the gradient norm  $\|\nabla\ell_i\|$ , the influence estimate  $\widehat{\Delta\ell}_i^{\text{IF}}$ , and the Newton estimate  $\widehat{\Delta\ell}_i^{\text{NS}}$ . Axes are log-log; the dotted diagonal  $y = x$  is the random baseline. Solid lines are means over 16 target models with  $\pm 1$  std bands; dashed-lines show a single representative model.

**Datasets and architectures.** We cover both classification and regression on tabular, vision and text data: (i) *CIFAR-10* with a small CNN; (ii) *CIFAR-100* with ResNet-20; (iii) *BloodMNIST* with a DINOv2 ViT-small classifier [Oquab et al., 2023], trained with a linear probe on top of frozen features; (iv) *SST-2* with a BERT [Devlin et al., 2019] classifier in two regimes: full fine-tuning of `bert_uncased_L-2_H-128_A-2` and a linear probe on top of a frozen `bert-base-uncased`; (v) *California Housing* with both a closed-form ridge regression and a deep MLP; (vi) *UCI Energy* with a tabular MLP. For each task we use the standard train split, randomly partitioned in half between members and non-members ( $N_{\text{train}} = N/2$ ) with a per-model seed, following the LiRA shadow-model protocol [Carlini et al., 2022a].

**Shadow and target models.** For every dataset/architecture pair we train 200 shadow (reference) models with i.i.d. random member/non-member splits, plus 16 independent target models used to compute the per-sample vulnerability surrogates. Optimizers, learning rates, batch sizes, weight decay and number of epochs follow standard recipes for each architecture (AdamW for vision and text, SGD-momentum for ResNet-20, Adam for the regression MLPs); the exact hyper-parameters are listed in Appendix C.1 and in the release scripts.

**Attacks and surrogates.** We use LiRA [Carlini et al., 2022a] as the reference per-sample attack, since it achieved the highest Attack Success Rate (ASR) in our experiments; we compute its per-sample ASR by averaging over the 200 reference models. We compare four *retraining-free* surrogates of vulnerability, all computed from a *single* target model and *without* shadow models: the training loss  $\ell_i$ , the gradient-norm  $\|\nabla\ell_i\|$ , the influence-function estimate  $\widehat{\Delta\ell}_i^{\text{IF}}$  and the Newton-step estimate  $\widehat{\Delta\ell}_i^{\text{NS}}$ .

For deep networks, both variants are restricted to the last layer, which keeps their cost essentially negligible. In Appendix D, we extend this analysis to include comparisons with both the RMIA attack [Zarifzadeh et al., 2024] and the original shadow-model attack [Shokri

Table 1: Recall (%) of the true LiRA top-1% when keeping the top-5% by each surrogate. Mean  $\pm$  std across target models. Higher is better; **bold** = best per dataset.

Dataset	Model	Recall of Top 1% @5% (in %)			
		Loss $\ell_i$	$\ \nabla\ell_i\ $	$\widehat{\Delta}_i^{\text{NS}}$	$\widehat{\Delta}_i^{\text{IF}}$
SST-2	BERT, full ft.	28.2 $\pm$ 2.4 %	5.3 $\pm$ 1.1 %	28.8 $\pm$ 2.6 %	<b>28.8 <math>\pm</math> 2.6 %</b>
	BERT, linear probe	<b>10.7 <math>\pm</math> 1.6 %</b>	7.2 $\pm$ 1.9 %	8.2 $\pm$ 2.5 %	8.9 $\pm$ 1.6 %
CalHousing	Ridge regression	12.3 $\pm$ 2.8 %	12.3 $\pm$ 2.8 %	<b>13.3 <math>\pm</math> 2.6 %</b>	13.2 $\pm$ 2.5 %
	MLP	52.2 $\pm$ 6.7 %	22.5 $\pm$ 6.9 %	74.9 $\pm$ 7.4 %	<b>75.5 <math>\pm</math> 7.0 %</b>
CIFAR-10	CNN	53.7 $\pm$ 2.5 %	36.8 $\pm$ 2.5 %	<b>62.8 <math>\pm</math> 2.1 %</b>	62.2 $\pm$ 2.2 %
CIFAR-100	ResNet-20	23.5 $\pm$ 1.5 %	12.3 $\pm$ 1.8 %	<b>36.8 <math>\pm</math> 5.1 %</b>	35.2 $\pm$ 4.6 %
BloodMNIST	DINOV2	74.3 $\pm$ 6.4 %	82.3 $\pm$ 3.9 %	<b>90.4 <math>\pm</math> 12.7 %</b>	87.1 $\pm$ 9.0 %
UCI Energy	MLP	12.5 $\pm$ 16.7 %	14.6 $\pm$ 21.0 %	33.3 $\pm$ 34.4 %	<b>39.6 <math>\pm</math> 32.7 %</b>

et al., 2017]. For two settings, CIFAR10 with a CNN and California Housing with an MLP, we additionally computed the full-network influence function estimate of the loss, without the restriction to the last layer, i.e.,  $\nabla_{\theta}\ell_i^{\top} H_{\theta}^{-1} \nabla_{\theta}\ell_i$ . We compute it using the inverse Hessian Products [Pearlmutter, 1994] and the Conjugate Gradient algorithm [Hestenes and Stiefel, 1952]. More details can be found in Appendix D.1.

**Metrics.** Following standard per-sample auditing practice [Shokri et al., 2017, Carlini et al., 2022a, Zarifzadeh et al., 2024], we evaluate surrogates based on top- $k$ % recall: the fraction of the most vulnerable points (highest ASR) correctly identified within the surrogate’s top- $k$ % rankings. The Spearman rank correlation is provided in Appendix D.2 for reference, but we find it less informative in our context as it is dominated by the high density of points near the 50% ASR (random guess), where surrogates provide little discriminative signal.

All experiments were run on an Nvidia-V100 GPU cluster; the full pipeline, training, statistics, attacks, scores and figures, is reproducible from the released code through the per-dataset launch scripts, and will be released publicly upon acceptance of the paper.

## 5.2 Results

We present the recall @5% of the true LiRA top-1% (measured by Average Success Rate) in Table 1. Figure 2 illustrates the performance of these surrogates for multiple recall percentages. We also present more extensive results for different percentages of recall in Appendix D, which show similar trends.

Across all eight settings, our two surrogates  $\widehat{\Delta}_i^{\text{IF}}$  and  $\widehat{\Delta}_i^{\text{NS}}$ , consistently recover the samples LiRA flags as most vulnerable, well above the random baseline, often by one to two orders of magnitude.

They also surpass the loss baseline on seven out of eight settings, with recall@1% improving by more than 20% on some datasets. The sole exception is the BERT linear probe, where the loss baseline marginally outperforms our method; we hypothesize that this setting, characterized by simple training dynamics and few vulnerable points, is one in which the raw loss already provides a strong signal. We further observe high variance in recall@1% across all surrogates on the UCI Energy dataset, which we attribute to the mismatch between the small dataset size ( $N = 768$ ) and the high-dimensional tabular MLP ( $p = 512$ ). At this scale, recall@1% is evaluated over only 7 points, making the metric inherently noisy.

Interestingly, our leverage-based surrogates have greater difficulty recovering the most vulnerable points for RMIA and Shokri classifier-based attacks (Appendix D.3). For RMIA, our method still outperforms the loss baseline in all cases, although by a narrower margin. For the classifier-based approach, this is likely because the attack learns a non-parametric decision boundary that is not well captured by the leverage-based scores, which are derived from a local quadratic approximation of the loss landscape. Finally, the full-network influence function proved worse in both speed and recall compared to our last-layer approach (see Appendix D.1).

Overall, these scores yield a shadow-free, single-model proxy that approaches LiRA’s per-point ASR ranking at a fraction of its computational cost. Scoring all points with our leverage-based surrogates on a single target model is  $1,000\times$  to  $10,000\times$  faster than training the 200 shadow models required by LiRA, excluding the target-model training cost, which is shared by both approaches. Detailed timings for each surrogate and attack are reported in the Appendix C.2.

## 6 Conclusion

We proposed a retraining-free framework for per-sample membership inference vulnerability assessment. In Gaussian linear regression, we derived a closed-form decomposition of the expected leave-one-out gap into a response-free population leverage term and a response-dependent structural error. We extended this view to deep networks via influence-function and Newton-step surrogates restricted to the last layer, both computable from a single trained model. Across eight dataset/architecture pairs, our surrogates outperform loss and gradient-norm baselines at recovering LiRA’s most vulnerable points, at a fraction of the cost.

Limitations remain: the theory is exact only in the linear case, the last-layer restriction overlooks earlier feature learning, and the surrogates track LiRA more closely than RMIA or classifier-based attacks. Natural extensions include layer-wise or kernel-based leverage scores, integration into DP-SGD training as a canary-selection or per-sample weighting tool, and a finer characterization of which memorization signals escape local quadratic approximations.

## References

- Martín Abadi, Andy Chu, Ian Goodfellow, H. Brendan McMahan, Ilya Mironov, Kunal Talwar, and Li Zhang. Deep Learning with Differential Privacy. In *Proceedings of the 2016 ACM SIGSAC Conference on Computer and Communications Security*, pages 308–318, October 2016.
- Mohammad Alaggan, Sébastien Gambs, and Anne-Marie Kermarrec. Heterogeneous differential privacy. *Journal of Privacy and Confidentiality*, 7(2), Jan. 2017.
- David M. Allen. The relationship between variable selection and data augmentation and a method for prediction. *Technometrics*, 16(1):125–127, 1974. ISSN 00401706.
- S Basu, P Pope, and S Feizi. Influence functions in deep learning are fragile. In *International Conference on Learning Representations (ICLR)*, 2021.
- David A Belsley, Edwin Kuh, and Roy E Welsch. *Regression Diagnostics: Identifying Influential Data and Sources of Collinearity*, chapter 2, pages 6–84. John Wiley & Sons, Ltd, 1980.
- Nicholas Carlini, Chang Liu, Úlfar Erlingsson, Jernej Kos, and Dawn Song. The secret sharer: Evaluating and testing unintended memorization in neural networks. In *28th USENIX security symposium (USENIX security 19)*, pages 267–284, 2019.
- Nicholas Carlini, Steve Chien, Milad Nasr, Shuang Song, Andreas Terzis, and Florian Tramèr. Membership inference attacks from first principles. In *2022 IEEE symposium on security and privacy (SP)*, pages 1897–1914. IEEE, 2022a.
- Nicholas Carlini, Matthew Jagielski, Chiyuan Zhang, Nicolas Papernot, Andreas Terzis, and Florian Tramèr. The privacy onion effect: Memorization is relative. *Advances in Neural Information Processing Systems*, 35:13263–13276, 2022b.
- Gilad Cohen and Raja Giryes. Membership Inference Attack Using Self Influence Functions. In *2024 IEEE/CVF Winter Conference on Applications of Computer Vision (WACV)*, pages 4880–4889, Waikoloa, HI, USA, January 2024. IEEE. ISBN 979-8-3503-1892-0.
- Jacob Devlin, Ming-Wei Chang, Kenton Lee, and Kristina Toutanova. Bert: Pre-training of deep bidirectional transformers for language understanding. In *Proceedings of the 2019 conference of the North American chapter of the association for computational linguistics: human language technologies, volume 1 (long and short papers)*, pages 4171–4186, 2019.
- C. Dwork. *Differential privacy*, volume 2006. ICALP, 2006.
- Vitaly Feldman. Does learning require memorization? a short tale about a long tail. In *Proceedings of the 52nd annual ACM SIGACT symposium on theory of computing*, pages 954–959, 2020.
- Vitaly Feldman and Chiyuan Zhang. What neural networks memorize and why: Discovering the long tail via influence estimation. *Advances in Neural Information Processing Systems*, 33:2881–2891, 2020.
- Chuan Guo, Tom Goldstein, Awni Hannun, and Laurens Van Der Maaten. Certified data removal from machine learning models. In Hal Daumé III and Aarti Singh, editors, *Proceedings of the 37th International Conference on Machine Learning*, volume 119 of *Proceedings of Machine Learning Research*, pages 3832–3842. PMLR, 13–18 Jul 2020.
- Frank R. Hampel. The influence curve and its role in robust estimation. *Journal of the American Statistical Association*, 69(346):383–393, 1974. ISSN 01621459, 1537274X.

- M.R. Hestenes and E. Stiefel. Methods of conjugate gradients for solving linear systems. *Journal of Research of the National Bureau of Standards*, 49(6):409, December 1952. ISSN 0091-0635.
- Matthew Jagielski, Jonathan Ullman, and Alina Oprea. Auditing differentially private machine learning: How private is private sgd? *Advances in Neural Information Processing Systems*, 33:22205–22216, 2020.
- Pang Wei Koh and Percy Liang. Understanding Black-box Predictions via Influence Functions. In *Proceedings of the 34th International Conference on Machine Learning*, pages 1885–1894. PMLR, July 2017.
- Mathias Lecuyer, Vaggelis Atlidakis, Roxana Geambasu, Daniel Hsu, and Suman Jana. Certified robustness to adversarial examples with differential privacy. In *2019 IEEE symposium on security and privacy (SP)*, pages 656–672. IEEE, 2019.
- Robb J. Muirhead. *The Multivariate Linear Model*, chapter 10, pages 429–525. John Wiley & Sons, Ltd, 1982. ISBN 9780470316559.
- Milad Nasr, Shuang Songi, Abhradeep Thakurta, Nicolas Papernot, and Nicholas Carlin. Adversary instantiation: Lower bounds for differentially private machine learning. In *2021 IEEE Symposium on security and privacy (SP)*, pages 866–882. IEEE, 2021.
- Jerzy Neyman and Egon Sharpe Pearson. Ix. on the problem of the most efficient tests of statistical hypotheses. *Philosophical Transactions of the Royal Society of London, Series A: Containing Papers of a Mathematical or Physical Character*, 231(694-706):289–337, 02 1933.
- Maxime Oquab, Timothée Darcet, Théo Moutakanni, Huy Vo, Marc Szafraniec, Vasil Khali-dov, Pierre Fernandez, Daniel Haziza, Francisco Massa, Alaaeldin El-Nouby, et al. Dinov2: Learning robust visual features without supervision. *arXiv preprint arXiv:2304.07193*, 2023.
- Barak A. Pearlmutter. Fast exact multiplication by the hessian. *Neural Computation*, 6(1): 147–160, 01 1994.
- Daryl Pregibon. Logistic regression diagnostics. *The Annals of Statistics*, 9(4):705–724, 1981.
- Ahmed Salem, Yang Zhang, Mathias Humbert, Pascal Berrang, Mario Fritz, and Michael Backes. MI-leaks: Model and data independent membership inference attacks and defenses on machine learning models. *arXiv preprint arXiv:1806.01246*, 2018.
- Ayush Sekhari, Jayadev Acharya, Gautam Kamath, and Ananda Theertha Suresh. Remember what you want to forget: Algorithms for machine unlearning. In M. Ranzato, A. Beygelzimer, Y. Dauphin, P.S. Liang, and J. Wortman Vaughan, editors, *Advances in Neural Information Processing Systems*, volume 34, pages 18075–18086. Curran Associates, Inc., 2021.
- Reza Shokri, Marco Stronati, Congzheng Song, and Vitaly Shmatikov. Membership inference attacks against machine learning models. In *2017 IEEE symposium on security and privacy (SP)*, pages 3–18. IEEE, 2017.
- Liwei Song and Prateek Mittal. Systematic evaluation of privacy risks of machine learning models. In *30th USENIX security symposium (USENIX security 21)*, pages 2615–2632, 2021.
- Anshuman Suri, Xiao Zhang, and David Evans. Do parameters reveal more than loss for membership inference? *Transactions on Machine Learning Research*, 2024.

- Jasper Tan, Blake Mason, Hamid Javadi, and Richard Baraniuk. Parameters or privacy: A provable tradeoff between overparameterization and membership inference. *Advances in Neural Information Processing Systems*, 35:17488–17500, 2022.
- Yu-Xiang Wang. Per-instance differential privacy, 2018. URL <https://arxiv.org/abs/1707.07708>.
- Samuel Yeom, Irene Giacomelli, Matt Fredrikson, and Somesh Jha. Privacy risk in machine learning: Analyzing the connection to overfitting. In *2018 IEEE 31st computer security foundations symposium (CSF)*, pages 268–282. IEEE, 2018.
- Sajjad Zarifzadeh, Philippe Liu, and Reza Shokri. Low-Cost High-Power Membership Inference Attacks. In Ruslan Salakhutdinov, Zico Kolter, Katherine Heller, Adrian Weller, Nuria Oliver, Jonathan Scarlett, and Felix Berkenkamp, editors, *Proceedings of the 41st International Conference on Machine Learning*. PMLR, 21–27 Jul 2024.
- Chiyuan Zhang, Samy Bengio, Moritz Hardt, Benjamin Recht, and Oriol Vinyals. Understanding deep learning requires rethinking generalization. In *International Conference on Learning Representations*, 2017.

# Table of Contents

<b>A Omitted Proofs from Section 3</b>	<b>15</b>
A.1 Proof of Lemma 3.1 (Joint Law of Leverage Scores and Residuals)	15
A.2 Proof of Proposition 3.2 (Per-sample Loss Distribution)	16
A.3 Proof of Corollary 3.3 (Optimal MIA Trade-off)	17
A.4 Proof of Proposition 3.4 (Expected Generalization Gap)	17
A.5 Generalization to the Multivariate Case	18
<b>B Omitted Proofs from Section 4</b>	<b>19</b>
B.1 Proof of the Influence Function Estimate (Eq. (7))	19
B.2 Proof of the Newton Step Estimate (Eq. (8))	20
B.3 Results in the Linear Regression (Eq. (9))	20
B.4 Results in the Logistic Regression (Eq. (10))	21
B.5 Proof that $\partial \hat{p}_i / \partial y_i = h_{ii}$	21
B.6 Generalization to the Multivariate Case	22
<b>C Details on the Experimental Setup</b>	<b>25</b>
C.1 Model Architectures and Training Hyperparameters	25
C.2 Time and Compute Resources	25
<b>D Additional Experimental Results</b>	<b>26</b>
D.1 Comparison with full-network Influence functions	26
D.2 Top- $k$ recall and Spearman correlation for LiRA attack	27
D.3 Top- $k$ recall and Spearman correlation for RMIA attack and Classifier Shokri's attack	27
D.4 Additional visualizations	27

## A Omitted Proofs from Section 3

This appendix provides the rigorous proofs for the theoretical results characterizing the finite-sample generalization gap. Throughout these proofs, we maintain the conditioning on the fixed target observation  $(x_i, y_i)$ , treating  $x_i$  and  $y_i$  as deterministic constants. The randomness originates entirely from  $X_{-i}$  and  $Y_{-i}$ .

### A.1 Proof of Lemma 3.1 (Joint Law of Leverage Scores and Residuals)

*Proof.* We first derive the distribution of the empirical leverage score  $h_{ii}$ . With  $G_{-i} = X_{-i}^\top X_{-i}$ , the full Gram matrix can be decomposed as  $X^\top X = G_{-i} + x_i x_i^\top$ . The empirical leverage score for the  $i$ -th observation is  $h_{ii} = x_i^\top (X^\top X)^{-1} x_i$ .

Applying the Sherman-Morrison formula to invert the rank-one update:

$$(G_{-i} + x_i x_i^\top)^{-1} = G_{-i}^{-1} - \frac{G_{-i}^{-1} x_i x_i^\top G_{-i}^{-1}}{1 + x_i^\top G_{-i}^{-1} x_i}$$

Multiplying both sides by  $x_i^\top$  on the left and  $x_i$  on the right yields:

$$h_{ii} = x_i^\top G_{-i}^{-1} x_i - \frac{(x_i^\top G_{-i}^{-1} x_i)^2}{1 + x_i^\top G_{-i}^{-1} x_i}$$

Let  $\tilde{h}_{ii} = x_i^\top G_{-i}^{-1} x_i$ . Simplifying the fraction, we obtain  $h_{ii} = \frac{\tilde{h}_{ii}}{1 + \tilde{h}_{ii}}$ .

Because the rows of  $X_{-i}$  are i.i.d.  $\mathcal{N}(0, \Sigma)$ ,  $G_{-i}$  follows a Wishart distribution  $\mathcal{W}_p(\Sigma, n-1)$ . A standard property of the Inverse-Wishart distribution states that for any fixed vector  $x_i$ , the quadratic form scales as an inverse chi-squared random variable. Specifically:

$$\frac{x_i^\top \Sigma^{-1} x_i}{x_i^\top G_{-i}^{-1} x_i} \sim \chi_{(n-1)-p+1}^2 = \chi_{n-p}^2$$

Let this random variable be denoted as  $V$ . Recalling that  $\bar{h}_{ii} = x_i^\top \Sigma^{-1} x_i$ , we have  $V = \bar{h}_{ii}/\tilde{h}_{ii}$ , which implies  $\tilde{h}_{ii} = \bar{h}_{ii}/V$ . Substituting this into our expression for  $h_{ii}$  gives:

$$h_{ii} = \frac{\bar{h}_{ii}/V}{1 + \bar{h}_{ii}/V} = \frac{\bar{h}_{ii}}{V + \bar{h}_{ii}}$$

which concludes the first part of the lemma.

We now derive the distribution of the leave-one-out residual  $e_{-i}$ . The leave-one-out OLS estimator is  $\hat{\theta}_{-i} = G_{-i}^{-1} X_{-i}^\top Y_{-i}$ . Under the true model,  $Y_{-i} = X_{-i} \theta + \varepsilon_{-i}$ , where  $\varepsilon_{-i} \sim \mathcal{N}(0, \sigma^2 I_{n-1})$  is unconditionally independent of  $X_{-i}$ . Substituting this yields  $\hat{\theta}_{-i} = \theta + G_{-i}^{-1} X_{-i}^\top \varepsilon_{-i}$ .

The leave-one-out residual is:

$$e_{-i} = y_i - x_i^\top \hat{\theta}_{-i} = (y_i - x_i^\top \theta) - x_i^\top G_{-i}^{-1} X_{-i}^\top \varepsilon_{-i} = \varepsilon_i - U$$

where  $\varepsilon_i = y_i - x_i^\top \theta$  is a deterministic constant and  $U = x_i^\top G_{-i}^{-1} X_{-i}^\top \varepsilon_{-i}$ .

We now condition on  $X_{-i}$ . Since  $\varepsilon_{-i} \perp\!\!\!\perp X_{-i}$ , the conditional distribution of  $\varepsilon_{-i}$  remains  $\mathcal{N}(0, \sigma^2 I_{n-1})$ . Because  $U$  is a linear combination of a Gaussian vector,  $U \mid X_{-i}$  is Gaussian. Its conditional moments are:

$$\mathbb{E}[U \mid X_{-i}] = x_i^\top G_{-i}^{-1} X_{-i}^\top \mathbb{E}[\varepsilon_{-i}] = 0 \quad (11)$$

$$\text{Var}(U \mid X_{-i}) = x_i^\top G_{-i}^{-1} X_{-i}^\top (\sigma^2 I_{n-1}) X_{-i} G_{-i}^{-1} x_i = \sigma^2 x_i^\top G_{-i}^{-1} G_{-i} G_{-i}^{-1} x_i = \sigma^2 \tilde{h}_{ii} \quad (12)$$

Substituting  $\tilde{h}_{ii} = \bar{h}_{ii}/V$ , we have  $U \mid X_{-i} \sim \mathcal{N}(0, \sigma^2 \bar{h}_{ii}/V)$ . Let  $Z = -U/(\sigma \sqrt{\bar{h}_{ii}}/\sqrt{V})$ . Then  $Z \mid X_{-i} \sim \mathcal{N}(0, 1)$ .

Crucially, because the conditional distribution of  $Z$  given  $X_{-i}$  is standard normal and does not depend on  $X_{-i}$ ,  $Z$  is unconditionally independent of  $X_{-i}$ . Since  $V$  is entirely a function of  $X_{-i}$ , it strictly follows that  $Z \perp\!\!\!\perp V$ . Thus, we can write the residual as  $e_{-i} = \varepsilon_i + \sigma \frac{\sqrt{\bar{h}_{ii}}}{\sqrt{V}} Z$ .

Finally, by standard regression update rules, the training residual is  $e_i = e_{-i}/(1 + \tilde{h}_{ii})$ . Squaring this yields the training loss:

$$\ell_i = e_i^2 = \left( \frac{e_{-i}}{1 + \tilde{h}_{ii}/V} \right)^2 = e_{-i}^2 \left( \frac{V}{V + \bar{h}_{ii}} \right)^2$$

□

## A.2 Proof of Proposition 3.2 (Per-sample Loss Distribution)

*Proof.* The results follow directly from Lemma 3.1 by writing that the training loss is

$$\ell_i = e_i^2 = e_{-i}^2 (1 - h_{ii})^2$$

and the leave-one-out loss is  $\ell_{-i} = e_{-i}^2$ .

□

### A.3 Proof of Corollary 3.3 (Optimal MIA Trade-off)

*Proof.* Under the non-member hypothesis  $\mathcal{H}_{\text{OUT}}$ , the optimal decision rule rejects the null hypothesis if the observed loss is unusually small:  $\ell_{\text{obs},i} < \gamma_\alpha$ . For a fixed False Positive Rate  $\alpha$ , the threshold is strictly determined by the non-member cumulative distribution function:  $\alpha = \mathbb{P}(\ell_{\text{obs},i} < \gamma_\alpha \mid \mathcal{H}_{\text{OUT}})$ , yielding  $\gamma_\alpha = F_{i,\text{OUT}}^{-1}(\alpha)$ .

Under the member hypothesis  $\mathcal{H}_{\text{IN}}$ , the loss is scaled by  $c_i^2$ . The True Positive Rate is the probability that this scaled loss falls below the same threshold:

$$\text{TPR}(\alpha) = \mathbb{P}(c_i^2 \ell_{\text{obs},i} < \gamma_\alpha \mid \mathcal{H}_{\text{OUT}}) = \mathbb{P}\left(\ell_{\text{obs},i} < \frac{\gamma_\alpha}{c_i^2} \mid \mathcal{H}_{\text{OUT}}\right) = F_{i,\text{OUT}}\left(\frac{\gamma_\alpha}{c_i^2}\right)$$

We finish the proof by writing  $\beta_i(\alpha) = \text{FNR}(\alpha) = 1 - \text{TPR}(\alpha)$  □

### A.4 Proof of Proposition 3.4 (Expected Generalization Gap)

*Proof.* The generalization gap is  $\Delta \ell_i = \ell_{-i} - \ell_i$ . Using the relationship  $\ell_i = e_{-i}^2 [V/(V + \bar{h}_{ii})]^2$ , we can factor out  $e_{-i}^2$ :

$$\Delta \ell_i = e_{-i}^2 \left(1 - \frac{V^2}{(V + \bar{h}_{ii})^2}\right) = e_{-i}^2 \left(\frac{(V + \bar{h}_{ii})^2 - V^2}{(V + \bar{h}_{ii})^2}\right) = e_{-i}^2 \frac{\bar{h}_{ii}(2V + \bar{h}_{ii})}{(V + \bar{h}_{ii})^2}$$

To compute the expectation  $\mathbb{E}[\Delta \ell_i \mid x_i, y_i]$ , we leverage the independence of  $Z$  and  $V$  established in Lemma 3.1. We first take the inner expectation with respect to  $Z$ :

$$\mathbb{E}_Z[e_{-i}^2 \mid V] = \mathbb{E}_Z \left[ \left( \varepsilon_i + \sigma \frac{\sqrt{\bar{h}_{ii}}}{\sqrt{V}} Z \right)^2 \right] \quad (13)$$

$$= \varepsilon_i^2 + 2\varepsilon_i \sigma \frac{\sqrt{\bar{h}_{ii}}}{\sqrt{V}} \mathbb{E}[Z] + \sigma^2 \frac{\bar{h}_{ii}}{V} \mathbb{E}[Z^2] = \varepsilon_i^2 + \sigma^2 \frac{\bar{h}_{ii}}{V} \quad (14)$$

Substituting this inner expectation into the gap yields the exact finite-sample formula:

$$\mathbb{E}[\Delta \ell_i \mid x_i, y_i] = \mathbb{E}_{V \sim \chi_{n-p}^2} \left[ \left( \varepsilon_i^2 + \sigma^2 \frac{\sqrt{\bar{h}_{ii}}}{V} \right) \frac{\bar{h}_{ii}(2V + \bar{h}_{ii})}{(V + \bar{h}_{ii})^2} \right]$$

To derive the asymptotic expansion, let  $k = n - p$  and define  $x = 1/V$ . We expand the rational term as  $x \rightarrow 0$  using the Maclaurin series for  $(1 + \bar{h}_{ii}x)^{-2}$ :

$$1 - (1 + \bar{h}_{ii}x)^{-2} = 1 - (1 - 2\bar{h}_{ii}x + 3\bar{h}_{ii}^2x^2 - \dots) = 2\bar{h}_{ii}x - 3\bar{h}_{ii}^2x^2 + \mathcal{O}(x^3)$$

Multiplying by the expanded residual term  $\mathbb{E}_Z[e_{-i}^2] = \varepsilon_i^2 + \sigma^2 \bar{h}_{ii}x$ :

$$\begin{aligned} g(x) &= (\varepsilon_i^2 + \sigma^2 \bar{h}_{ii}x)(2\bar{h}_{ii}x - 3\bar{h}_{ii}^2x^2 + \mathcal{O}(x^3)) \\ &= 2\varepsilon_i^2 \bar{h}_{ii}x + \bar{h}_{ii}^2(2\sigma^2 - 3\varepsilon_i^2)x^2 + \mathcal{O}(x^3) \end{aligned} \quad (15)$$

We now apply the exact inverse moments of the chi-squared distribution  $V \sim \chi_k^2$ . For  $k > 4$ :

$$\mathbb{E}[x] = \mathbb{E}[V^{-1}] = \frac{1}{k-2}, \quad \mathbb{E}[x^2] = \mathbb{E}[V^{-2}] = \frac{1}{(k-2)(k-4)}$$

Substituting these moments into our expansion:

$$\mathbb{E}[\Delta \ell_i] = \frac{2\varepsilon_i^2 \bar{h}_{ii}}{k-2} + \frac{\bar{h}_{ii}^2(2\sigma^2 - 3\varepsilon_i^2)}{(k-2)(k-4)} + \mathcal{O}(k^{-3})$$

Finally, we convert this falling-factorial series into standard powers of  $1/k$  using geometric series expansions:  $(k-2)^{-1} = k^{-1} + 2k^{-2} + \mathcal{O}(k^{-3})$  and  $(k-2)^{-1}(k-4)^{-1} = k^{-2} + \mathcal{O}(k^{-3})$ . Gathering like terms gives:

$$\begin{aligned}\mathbb{E}[\Delta\ell_i] &= 2\varepsilon_i^2\bar{h}_{ii}\left(\frac{1}{k} + \frac{2}{k^2}\right) + \bar{h}_{ii}^2(2\sigma^2 - 3\varepsilon_i^2)\left(\frac{1}{k^2}\right) + \mathcal{O}\left(\frac{1}{k^3}\right) \\ &= \frac{2\varepsilon_i^2\bar{h}_{ii}}{k} + \frac{4\varepsilon_i^2\bar{h}_{ii} + \bar{h}_{ii}^2(2\sigma^2 - 3\varepsilon_i^2)}{k^2} + \mathcal{O}\left(\frac{1}{k^3}\right)\end{aligned}\quad (16)$$

Substituting  $k = n - p$  completes the proof.  $\square$

## A.5 Generalization to the Multivariate Case

We now extend Proposition 3.4 to a  $q$ -dimensional response. Let  $Y_j \in \mathbb{R}^q$  be generated as  $Y_j | X_j \sim \mathcal{N}(\Theta^\top X_j, \Sigma_y)$  with  $\Theta \in \mathbb{R}^{p \times q}$  and  $\Sigma_y \succ 0$ . We collect responses in  $Y \in \mathbb{R}^{n \times q}$ , fit the OLS estimator  $\hat{\Theta} = (X^\top X)^{-1} X^\top Y$ , and define the training and leave-one-out losses

$$\ell_i = \|y_i - \hat{\Theta}^\top x_i\|^2, \quad \ell_{-i} = \|y_i - \hat{\Theta}_{-i}^\top x_i\|^2.$$

The structural error is now a vector  $\varepsilon_i = y_i - \Theta^\top x_i \in \mathbb{R}^q$ .

**Proposition A.1** (Multivariate generalization gap). *For  $n - p > 2$ , conditional on  $(x_i, y_i)$ ,*

$$\mathbb{E}[\Delta\ell_i | x_i, y_i] = \mathbb{E}_{V \sim \chi_{n-p}^2} \left[ \left( \|\varepsilon_i\|^2 + \text{tr}(\Sigma_y) \frac{\bar{h}_{ii}}{V} \right) \frac{\bar{h}_{ii}(2V + \bar{h}_{ii})}{(V + \bar{h}_{ii})^2} \right], \quad (17)$$

with the asymptotic expansion in  $k = n - p$

$$\mathbb{E}[\Delta\ell_i | x_i, y_i] = \frac{2\|\varepsilon_i\|^2\bar{h}_{ii}}{n-p} + \frac{4\|\varepsilon_i\|^2\bar{h}_{ii} + \bar{h}_{ii}^2(2\text{tr}(\Sigma_y) - 3\|\varepsilon_i\|^2)}{(n-p)^2} + \mathcal{O}\left(\frac{1}{(n-p)^3}\right). \quad (18)$$

*Proof.* The leverage analysis of Lemma 3.1 depends only on  $X$  and is unchanged:  $h_{ii} = \bar{h}_{ii}/(V + \bar{h}_{ii})$  with  $V \sim \chi_{n-p}^2$  and  $\bar{h}_{ii} = x_i^\top \Sigma^{-1} x_i$ .

Writing  $E = Y - X\Theta \in \mathbb{R}^{n \times q}$  for the noise matrix (rows i.i.d.  $\mathcal{N}(0, \Sigma_y)$ ), we have  $\hat{\Theta}_{-i} = \Theta + G_{-i}^{-1} X_{-i}^\top E_{-i}$ , hence

$$e_{-i} = y_i - \hat{\Theta}_{-i}^\top x_i = \varepsilon_i - U, \quad U = E_{-i}^\top X_{-i} G_{-i}^{-1} x_i \in \mathbb{R}^q.$$

Conditional on  $X_{-i}$ ,  $U$  is a linear combination of the independent rows of  $E_{-i}$ , hence Gaussian with  $\mathbb{E}[U | X_{-i}] = 0$  and

$$\text{Cov}(U | X_{-i}) = (x_i^\top G_{-i}^{-1} X_{-i}^\top X_{-i} G_{-i}^{-1} x_i) \Sigma_y = \tilde{h}_{ii} \Sigma_y = \frac{\bar{h}_{ii}}{V} \Sigma_y,$$

using  $\tilde{h}_{ii} = \bar{h}_{ii}/V$  from the proof of Lemma 3.1. Setting  $Z = -\sqrt{V}/\bar{h}_{ii} \cdot U$ , we obtain  $Z | X_{-i} \sim \mathcal{N}(0, \Sigma_y)$ . Since this conditional law does not depend on  $X_{-i}$ ,  $Z$  is unconditionally independent of  $X_{-i}$  and therefore of  $V$ . We thus write

$$e_{-i} = \varepsilon_i + \frac{\bar{h}_{ii}}{\sqrt{V}} Z, \quad Z \sim \mathcal{N}(0, \Sigma_y), \quad V \sim \chi_{n-p}^2, \quad Z \perp\!\!\!\perp V.$$

The univariate Sherman-Morrison contraction  $e_i = (1 - h_{ii})e_{-i}$  applies column-wise to  $\hat{\Theta}$ , so it carries over to vector residuals and yields  $\ell_i = (1 - h_{ii})^2 \ell_{-i}$ .

Combining the two displays,

$$\Delta\ell_i = \ell_{-i}(1 - (1 - h_{ii})^2) = \|e_{-i}\|^2 \cdot \frac{\bar{h}_{ii}(2V + \bar{h}_{ii})}{(V + \bar{h}_{ii})^2}.$$

By independence of  $Z$  and  $V$ ,

$$\mathbb{E}_Z[\|e_{-i}\|^2 | V] = \|\varepsilon_i\|^2 + 2 \frac{\bar{h}_{ii}}{\sqrt{V}} \varepsilon_i^\top \mathbb{E}[Z] + \frac{\bar{h}_{ii}}{V} \mathbb{E}[Z^\top Z] = \|\varepsilon_i\|^2 + \text{tr}(\Sigma_y) \frac{\bar{h}_{ii}}{V},$$

which yields the exact finite-sample expression in the proposition. The asymptotic expansion follows the same algebra as the proof of Theorem 3.4, replacing  $\varepsilon_i^2$  by  $\|\varepsilon_i\|^2$  and  $\sigma^2$  by  $\text{tr}(\Sigma_y)$ .  $\square$

The univariate result of Proposition 3.4 is recovered when  $q = 1$  and  $\Sigma_y = \sigma^2$ . Crucially, the leverage  $\bar{h}_{ii}$  remains label-free and so retains the same first-order role; only the structural-noise contribution is replaced by the sum of marginal output variances  $\text{tr}(\Sigma_y)$ .

## B Omitted Proofs from Section 4

### B.1 Proof of the Influence Function Estimate (Eq. (7))

We recall here the derivation of the influence function estimate, following the perturbation-based approach introduced by Koh and Liang [2017].

*Proof.* Let the empirical risk over the full dataset be  $R(\theta) = \frac{1}{n} \sum_{j=1}^n \ell(\theta, z_j)$ , and let  $\hat{\theta} = \arg \min_{\theta} R(\theta)$  be the empirical risk minimizer.

Rather than strictly removing the  $i$ -th point, we consider the effect of infinitesimally up-weighting the loss of  $z_i$  by some small continuous value  $\epsilon$ . We define the perturbed empirical risk minimizer as:

$$\hat{\theta}_{\epsilon, z_i} \triangleq \arg \min_{\theta} \left( \frac{1}{n} \sum_{j=1}^n \ell(\theta, z_j) + \epsilon \ell(\theta, z_i) \right)$$

By the first-order optimality condition, the gradient of the perturbed objective at  $\hat{\theta}_{\epsilon, z_i}$  must be zero:

$$0 = \frac{1}{n} \sum_{j=1}^n \nabla_{\theta} \ell(\hat{\theta}_{\epsilon, z_i}, z_j) + \epsilon \nabla_{\theta} \ell(\hat{\theta}_{\epsilon, z_i}, z_i)$$

We then differentiate this entire condition with respect to  $\epsilon$  and evaluate it at  $\epsilon = 0$  (where  $\hat{\theta}_{\epsilon, z_i} = \hat{\theta}$ ). Applying the chain rule yields:

$$0 = \left[ \frac{1}{n} \sum_{j=1}^n \nabla_{\theta}^2 \ell(\hat{\theta}, z_j) \right] \frac{d\hat{\theta}_{\epsilon, z_i}}{d\epsilon} \Big|_{\epsilon=0} + \nabla_{\theta} \ell(\hat{\theta}, z_i)$$

Let  $H = \frac{1}{n} \sum_{j=1}^n \nabla_{\theta}^2 \ell(\hat{\theta}, z_j)$  be the Hessian of the empirical risk. Solving for the derivative gives us the influence of up-weighting  $z_i$  on the parameters:

$$\mathcal{I}_{\text{up, params}}(z_i) \triangleq \frac{d\hat{\theta}_{\epsilon, z_i}}{d\epsilon} \Big|_{\epsilon=0} = -H^{-1} \nabla_{\theta} \ell(\hat{\theta}, z_i)$$

Removing the point  $z_i$  from the dataset corresponds to reducing its weight from  $\frac{1}{n}$  to 0. We can approximate this by setting  $\epsilon = -\frac{1}{n}$ . Using a first-order Taylor expansion around  $\epsilon = 0$ , the change in the parameters is:

$$\hat{\theta}_{-i} - \hat{\theta} \approx \left. \frac{d\hat{\theta}_{\epsilon, z_i}}{d\epsilon} \right|_{\epsilon=0} \cdot \left( -\frac{1}{n} \right) = \frac{1}{n} H^{-1} \nabla_{\theta} \ell(\hat{\theta}, z_i)$$

Finally, to estimate the loss gap for the  $i$ -th point, we apply a first-order Taylor expansion to the loss function itself:

$$\ell_{-i} - \ell_i \approx \nabla_{\theta} \ell(\hat{\theta}, z_i)^{\top} (\hat{\theta}_{-i} - \hat{\theta}) \approx \frac{1}{n} \nabla_{\theta} \ell(\hat{\theta}, z_i)^{\top} H^{-1} \nabla_{\theta} \ell(\hat{\theta}, z_i).$$

Expanding the Hessian  $H$  and pulling the factor  $n$  out of the inverse gives the final influence function estimate:

$$\Delta \ell_i \approx \nabla_{\theta} \ell(\hat{\theta}, z_i)^{\top} \left[ \sum_{j=1}^n \nabla_{\theta}^2 \ell(\hat{\theta}, z_j) \right]^{-1} \nabla_{\theta} \ell(\hat{\theta}, z_i)$$

This gives us our influence function estimate for the loss gap  $\widehat{\Delta \ell}_i^{\text{IF}}$  when removing the  $i$ -th point from the training set.  $\square$

## B.2 Proof of the Newton Step Estimate (Eq. (8))

*Proof.* The Newton step estimate is derived from the second-order Taylor expansion of the loss function around the empirical risk minimizer  $\hat{\theta}$ . The change in parameters when removing the  $i$ -th point can be approximated by the Newton update:

$$\hat{\theta}_{-i} - \hat{\theta} \approx -\nabla_{\theta}^2 \ell(\hat{\theta}, z_i)^{-1} \nabla_{\theta} \ell(\hat{\theta}, z_i)$$

This is equivalent to performing a single Newton step on the loss of the  $i$ -th point, treating it as a separate optimization problem. The estimated loss gap is then:

$$\Delta \ell_i \approx \ell_i(\hat{\theta} - \nabla_{\theta}^2 \ell(\hat{\theta}, z_i)^{-1} \nabla_{\theta} \ell(\hat{\theta}, z_i)) - \ell_i(\hat{\theta})$$

which gives our Newton step estimate for the loss gap  $\widehat{\Delta \ell}_i^{\text{NS}}$  for the point  $z_i$ .  $\square$

This estimate captures the curvature of the loss landscape around  $\hat{\theta}$  for the specific point  $z_i$ , and can provide a more accurate approximation of the loss gap compared to the influence function, especially when the loss is highly non-linear or when the Hessian is not well-conditioned.

## B.3 Results in the Linear Regression (Eq. (9))

We specialize Eq. (7) and Eq. (8) to the squared loss  $\ell(\theta, z_j) = (y_j - x_j^{\top} \theta)^2$  on the dataset  $\{(x_j, y_j)\}_{j=1}^n$ . Throughout,  $e_i = y_i - x_i^{\top} \hat{\theta}$  denotes the training residual and  $h_{ii} = x_i^{\top} (X^{\top} X)^{-1} x_i$  the leverage score.

*Proof.* For each  $j$ ,

$$\nabla_{\theta} \ell(\theta, z_j) = -2(y_j - x_j^{\top} \theta) x_j, \quad \nabla_{\theta}^2 \ell(\theta, z_j) = 2 x_j x_j^{\top}.$$

Evaluated at  $\hat{\theta}$ ,  $\nabla_{\theta} \ell(\hat{\theta}, z_i) = -2e_i x_i$ .

**Influence.** The full-data Hessian is  $\sum_{j=1}^n \nabla_{\theta}^2 \ell(\hat{\theta}, z_j) = 2 X^{\top} X$ . Substituting in Eq. (7):

$$\widehat{\Delta \ell}_i^{\text{IF}} = (-2e_i x_i)^{\top} (2 X^{\top} X)^{-1} (-2e_i x_i) = 2 e_i^2 x_i^{\top} (X^{\top} X)^{-1} x_i = 2 e_i^2 h_{ii}.$$

**Newton.** The leave-one-out Hessian is  $\sum_{j \neq i} \nabla_{\theta}^2 \ell(\hat{\theta}, z_j) = 2(X^{\top} X - x_i x_i^{\top}) = 2G_{-i}$ . Sherman-Morrison gives

$$x_i^{\top} G_{-i}^{-1} x_i \frac{x_i^{\top} (X^{\top} X)^{-1} x_i}{1 - x_i^{\top} (X^{\top} X)^{-1} x_i} = \frac{h_{ii}}{1 - h_{ii}}.$$

Substituting in Eq. (8):

$$\widehat{\Delta \ell}_i^{\text{NS}} = (-2e_i x_i)^{\top} (2G_{-i})^{-1} (-2e_i x_i) = 2 e_i^2 \cdot \frac{h_{ii}}{1 - h_{ii}}.$$

The Newton estimate is exact up to the first-order Taylor expansion of the loss; for the quadratic OLS loss, the second-order remainder is itself  $e_i^2 h_{ii}^2 / (1 - h_{ii})^2$ , recovering the exact leave-one-out identity  $\ell_{-i} = e_i^2 / (1 - h_{ii})^2$ .  $\square$

## B.4 Results in the Logistic Regression (Eq. (10))

We specialize Eq. (7) and Eq. (8) to the binary cross-entropy loss with  $\hat{p}_j = \sigma(x_j^{\top} \hat{\theta})$  and  $w_j = \hat{p}_j(1 - \hat{p}_j)$ . Let  $W = \text{diag}(w_j)_{j=1}^n$  and define the leverage score for the logistic model [Pregibon, 1981] as:

$$h_{ii} = w_i x_i^{\top} (X^{\top} W X)^{-1} x_i.$$

*Proof.* The per-sample loss  $\ell(\theta, z_j) = -y_j \log \hat{p}_j - (1 - y_j) \log(1 - \hat{p}_j)$  has gradient and Hessian

$$\nabla_{\theta} \ell(\theta, z_j) = -(y_j - \hat{p}_j) x_j, \quad \nabla_{\theta}^2 \ell(\theta, z_j) = w_j x_j x_j^{\top},$$

so the empirical Hessian is  $\sum_{j=1}^n \nabla_{\theta}^2 \ell(\hat{\theta}, z_j) = X^{\top} W X$ .

**Influence.** Substituting in Eq. (7):

$$\widehat{\Delta \ell}_i^{\text{IF}} = (y_i - \hat{p}_i)^2 x_i^{\top} (X^{\top} W X)^{-1} x_i = \frac{(y_i - \hat{p}_i)^2}{w_i} h_{ii}.$$

**Newton.** The leave-one-out Hessian is  $X^{\top} W X - w_i x_i x_i^{\top}$ . By Sherman-Morrison,

$$x_i^{\top} (X^{\top} W X - w_i x_i x_i^{\top})^{-1} x_i = \frac{x_i^{\top} (X^{\top} W X)^{-1} x_i}{1 - w_i x_i^{\top} (X^{\top} W X)^{-1} x_i} = \frac{h_{ii}/w_i}{1 - h_{ii}}.$$

Substituting in Eq. (8):

$$\widehat{\Delta \ell}_i^{\text{NS}} = (y_i - \hat{p}_i)^2 \cdot \frac{h_{ii}/w_i}{1 - h_{ii}} = \frac{(y_i - \hat{p}_i)^2}{w_i} \cdot \frac{h_{ii}}{1 - h_{ii}}.$$

$\square$

## B.5 Proof that $\partial \hat{p}_i / \partial y_i = h_{ii}$

*Proof.* The MLE  $\hat{\theta}$  satisfies the score equation

$$X^{\top} (y - \hat{p}) = 0,$$

where  $\hat{p} = \sigma(X\hat{\theta})$ . Differentiating with respect to  $y_i$  and applying the chain rule, with  $\partial\hat{p}/\partial\hat{\eta} = W$  and  $\hat{\eta} = X\hat{\theta}$ , yields

$$x_i = X^\top W X \frac{\partial\hat{\theta}}{\partial y_i}, \quad \text{hence} \quad \frac{\partial\hat{\theta}}{\partial y_i} = (X^\top W X)^{-1} x_i.$$

Since  $\partial\hat{p}_i/\partial y_i = w_i \partial\hat{\eta}_i/\partial y_i = w_i x_i^\top (\partial\hat{\theta}/\partial y_i)$ , we obtain

$$\frac{\partial\hat{p}_i}{\partial y_i} = w_i x_i^\top (X^\top W X)^{-1} x_i = h_{ii}. \quad \square$$

## B.6 Generalization to the Multivariate Case

We extend the closed-form expressions to multivariate-output settings: multivariate linear regression and multinomial logistic regression. The arguments rely only on the per-sample gradient and Hessian, so Eq. (7) and Eq. (8) apply. We derive the exact formulas for the influence and Newton estimates in these two cases.

**Multivariate linear regression.** For multivariate linear regression over  $q$  outputs with quadratic loss  $\ell(\Theta) = \sum_{j=1}^n \|y_j - \Theta^\top x_j\|^2$ , the problem decouples into  $q$  independent OLS regressions. For a single dimension  $k$ , the residual is  $e_{i,k} \in \mathbb{R}$ , the gradient is  $g_{i,k} = -2e_{i,k}x_i$ , and the scalar leverage is  $h_{ii} = x_i^\top (X^\top X)^{-1} x_i$ .

**Proposition B.1** (Influence Approximation). *The influence approximation (using the full-data Hessian) for the leave-one-out change in loss is:*

$$\widehat{\Delta\ell}_i^{\text{IF}} = 2\|e_i\|^2 h_{ii} \quad (19)$$

where  $e_i = y_i - \hat{\Theta}^\top x_i \in \mathbb{R}^q$  is the full residual vector.

*Proof.* The full Hessian for dimension  $k$  is  $\mathcal{H}_\Theta = 2X^\top X$  and is independent of  $k$ . The loss gap for dimension  $k$  using the influence approximation presented in equation\* (7) is:

$$\widehat{\Delta\ell}_{ik}^{\text{IF}} = g_{i,k}^\top \mathcal{H}_\Theta^{-1} g_{i,k} = (-2e_{i,k}x_i)^\top (2X^\top X)^{-1} (-2e_{i,k}x_i) = 2e_{i,k}^2 x_i^\top (X^\top X)^{-1} x_i = 2e_{i,k}^2 h_{ii}$$

Summing the independent changes over all  $q$  dimensions yields the total loss gap:

$$\widehat{\Delta\ell}_i^{\text{IF}} = \sum_{k=1}^q 2e_{i,k}^2 h_{ii} = 2h_{ii} \sum_{k=1}^q e_{i,k}^2 = 2\|e_i\|^2 h_{ii} \quad \square$$

**Proposition B.2** (Newton Approximation). *The Newton approximation, using the leave-one-out Hessian for the leave-one-out change in loss is:*

$$\widehat{\Delta\ell}_i^{\text{NS}} = 2\|e_i\|^2 \frac{h_{ii}}{1-h_{ii}} \quad (20)$$

*Proof.* The exact LOO Hessian for dimension  $k$  is  $H_{-i} = 2(X^\top X - x_i x_i^\top)$ . Applying the Sherman-Morrison formula to invert this rank-1 downdate yields  $x_i^\top (X^\top X - x_i x_i^\top)^{-1} x_i = \frac{h_{ii}}{1-h_{ii}}$ . The loss gap per dimension using this LOO Hessian is:

$$\widehat{\Delta\ell}_{ik}^{\text{NS}} = g_{i,k}^\top H_{-i}^{-1} g_{i,k} = (-2e_{i,k}x_i)^\top [2(X^\top X - x_i x_i^\top)]^{-1} (-2e_{i,k}x_i)$$

$$\widehat{\Delta\ell}_{ik}^{\text{NS}} = 4e_{i,k}^2 \cdot \frac{1}{2} x_i^\top (X^\top X - x_i x_i^\top)^{-1} x_i = 2e_{i,k}^2 \frac{h_{ii}}{1 - h_{ii}}$$

Summing over all  $q$  dimensions yields the total loss gap:

$$\widehat{\Delta\ell}_i^{\text{NS}} = \sum_{k=1}^q 2e_{i,k}^2 \frac{h_{ii}}{1 - h_{ii}} = 2 \frac{h_{ii}}{1 - h_{ii}} \sum_{k=1}^q e_{i,k}^2 = 2\|e_i\|^2 \frac{h_{ii}}{1 - h_{ii}}$$

□

**Multivariate logistic regression.** We denote  $y_j \in \{0, 1\}^m$  the one-hot encoded label,  $\hat{\Theta} \in \mathbb{R}^{p \times m}$  the learned parameter, and  $\ell_j(\hat{\Theta}) = -\sum_{k=1}^m y_{jk} \log \hat{p}_{jk}$  the total loss, with  $\hat{p}_j = \text{softmax}(\hat{\Theta}^\top x_j)$  the predicted class probabilities. The results for the influence and Newton estimates are given in the following proposition.

**Proposition B.3.** *In the multivariate case for multinomial logistic regression over  $m$  classes, we have:*

$$\widehat{\Delta\ell}_i^{\text{NS}} = g_i^\top H_{ii} (I_m - W_i H_{ii})^{-1} g_i \quad (21)$$

Where

- $g_i = \hat{p}_i - y_i \in \mathbb{R}^m$ .
- $W_i = \text{diag}(\hat{p}_i) - \hat{p}_i \hat{p}_i^\top \in \mathbb{R}^{m \times m}$ .
- $H_{ii} = \tilde{X}_i^\top \mathcal{H}_{\hat{\Theta}}^{-1} \tilde{X}_i \in \mathbb{R}^{m \times m}$  is the block-diagonal leverage matrix.
- $\tilde{X}_i = x_i \otimes I_m \in \mathbb{R}^{pm \times m}$  is the expanded feature matrix.
- $\mathcal{H}_{\hat{\Theta}} = \sum_{j=1}^n x_j x_j^\top \otimes W_j \in \mathbb{R}^{pm \times pm}$  is the full Hessian of the loss.

*Proof.* Let  $L(\hat{\Theta}) = \sum_{j=1}^n \ell_j(\hat{\Theta})$  be the total cross-entropy loss. For convenience, we parameterize the model by the vectorized weights  $\hat{\Theta} \in \mathbb{R}^{pm}$  instead of a matrix  $\in \mathbb{R}^{p \times m}$ . Using the provided definitions, the per-sample gradient and Hessian evaluated at the optimal full-data parameters  $\hat{\Theta}$  can be written compactly as:

$$\nabla_{\hat{\Theta}} \ell_i(\hat{\Theta}) = \tilde{X}_i g_i$$

$$\nabla_{\hat{\Theta}}^2 \ell_i(\hat{\Theta}) = \tilde{X}_i W_i \tilde{X}_i^\top = (x_i \otimes I_m) W_i (x_i^\top \otimes I_m) = x_i x_i^\top \otimes W_i$$

Summing the per-sample Hessians gives the full Hessian  $\mathcal{H}_{\hat{\Theta}} = \sum_{j=1}^n \tilde{X}_j W_j \tilde{X}_j^\top$ . When we leave out the  $i$ -th sample, the leave-one-out Hessian  $\mathcal{H}_{-i}$  is defined as:

$$\mathcal{H}_{-i} = \mathcal{H}_{\hat{\Theta}} - \tilde{X}_i W_i \tilde{X}_i^\top$$

Using a single Newton step approximation, the change in the estimated parameters upon removing the  $i$ -th sample is:

$$\Delta \hat{\Theta}_i \approx \mathcal{H}_{-i}^{-1} \nabla_{\hat{\Theta}} \ell_i(\hat{\Theta}) = \mathcal{H}_{-i}^{-1} \tilde{X}_i g_i$$

The approximate change in the loss function for the left-out sample,  $\Delta \ell_i$ , evaluates the gradient against this parameter shift:

$$\Delta \ell_i \approx \nabla_{\hat{\Theta}} \ell_i(\hat{\Theta})^\top \Delta \hat{\Theta}_i = (\tilde{X}_i g_i)^\top \mathcal{H}_{-i}^{-1} (\tilde{X}_i g_i) = g_i^\top \left( \tilde{X}_i^\top \mathcal{H}_{-i}^{-1} \tilde{X}_i \right) g_i$$

To evaluate the inner term without explicitly inverting the  $pm \times pm$  LOO Hessian, we apply the Woodbury matrix identity to  $\mathcal{H}_{-i}^{-1} = (\mathcal{H}_{\hat{\Theta}} - \tilde{X}_i W_i \tilde{X}_i^\top)^{-1}$ . Because the weight matrix  $W_i$  is not strictly invertible (its columns sum to zero), we use the form of the Woodbury identity that does not require  $W_i^{-1}$ :

$$(\mathcal{H}_{\hat{\Theta}} - \tilde{X}_i W_i \tilde{X}_i^\top)^{-1} = \mathcal{H}_{\hat{\Theta}}^{-1} + \mathcal{H}_{\hat{\Theta}}^{-1} \tilde{X}_i W_i (I_m - \tilde{X}_i^\top \mathcal{H}_{\hat{\Theta}}^{-1} \tilde{X}_i W_i)^{-1} \tilde{X}_i^\top \mathcal{H}_{\hat{\Theta}}^{-1}$$

We substitute this expanded inverse into our target expression  $\tilde{X}_i^\top \mathcal{H}_{-i}^{-1} \tilde{X}_i$ . Leveraging the definition  $H_{ii} = \tilde{X}_i^\top \mathcal{H}_{\hat{\Theta}}^{-1} \tilde{X}_i$ , we obtain:

$$\tilde{X}_i^\top \mathcal{H}_{-i}^{-1} \tilde{X}_i = H_{ii} + H_{ii} W_i (I_m - H_{ii} W_i)^{-1} H_{ii}$$

Next, we factor out  $H_{ii}$  on the left side:

$$\tilde{X}_i^\top \mathcal{H}_{-i}^{-1} \tilde{X}_i = H_{ii} [I_m + W_i (I_m - H_{ii} W_i)^{-1} H_{ii}]$$

Applying the push-through matrix identity  $W_i (I_m - H_{ii} W_i)^{-1} = (I_m - W_i H_{ii})^{-1} W_i$ , the term inside the brackets becomes:

$$\tilde{X}_i^\top \mathcal{H}_{-i}^{-1} \tilde{X}_i = H_{ii} [I_m + (I_m - W_i H_{ii})^{-1} W_i H_{ii}]$$

To combine these terms, we multiply the identity matrix  $I_m$  by  $(I_m - W_i H_{ii})^{-1} (I_m - W_i H_{ii})$ :

$$\tilde{X}_i^\top \mathcal{H}_{-i}^{-1} \tilde{X}_i = H_{ii} [(I_m - W_i H_{ii})^{-1} (I_m - W_i H_{ii}) + (I_m - W_i H_{ii})^{-1} W_i H_{ii}]$$

Factoring out  $(I_m - W_i H_{ii})^{-1}$  from both terms in the bracket leaves:

$$\tilde{X}_i^\top \mathcal{H}_{-i}^{-1} \tilde{X}_i = H_{ii} (I_m - W_i H_{ii})^{-1} (I_m - W_i H_{ii} + W_i H_{ii})$$

The  $-W_i H_{ii}$  and  $+W_i H_{ii}$  cleanly cancel out, yielding the final simplified matrix expression:

$$\tilde{X}_i^\top \mathcal{H}_{-i}^{-1} \tilde{X}_i = H_{ii} (I_m - W_i H_{ii})^{-1}$$

Substituting this matrix back into our earlier equation for the scalar change in loss yields the desired formulation:

$$\widehat{\Delta \ell}_i^{\text{NS}} = g_i^\top H_{ii} (I_m - W_i H_{ii})^{-1} g_i$$

□

**Proposition B.4.** *In the multivariate case for multinomial logistic regression over  $m$  classes, we have*

$$\widehat{\Delta \ell}_i^{\text{IF}} = g_i^\top H_{ii} g_i \quad (22)$$

Where  $g_i$ ,  $H_{ii}$  are defined as in the previous proposition.

*Proof.* The influence function approximation is a special case of the Newton step approximation where we take only the first-order term in the Taylor expansion of the loss. This corresponds to replacing the matrix inverse  $(I_m - W_i H_{ii})^{-1}$  with the identity matrix  $I_m$ . □

For  $m = 2$  the per-sample weight collapses to the scalar  $w_j$ ,  $\mathcal{H}_{\hat{\Theta}} = X^\top W X$  factorizes as a single Kronecker product, and we recover the binary formulas of the previous subsection. In general  $\mathcal{H}$  does *not* factorize as a Kronecker product because  $W_j$  depends on  $j$ , so the multinomial leverage cannot be separated into a sample term and a class term as in the binary case.

## C Details on the Experimental Setup

### C.1 Model Architectures and Training Hyperparameters

We evaluate our surrogates on a deliberately diverse benchmark spanning tabular regression, image classification, and text classification, with model sizes ranging from a single linear layer to a fully fine-tuned transformer. For each (dataset, architecture) pair, target and reference (shadow) models are trained with the *same* hyperparameters; only the random seed, which controls both weight initialization and the training split differs. We train 200 reference models and 16 target models per setting. Table 2 summarizes the architectures and Table 3 the training hyperparameters. The detailed implementation can be found in the codebase.

Table 2: Datasets and architectures used in our benchmark.  $|\mathcal{D}|$  denotes the number of training examples used to draw membership splits. #classes is only relevant for classification tasks.

Dataset	Task	Model	Backbone	$ \mathcal{D} $	#classes
UCI Energy	Reg.	MLP	2 hidden blocks [64, 32], dropout 0.3	614	—
California Housing	Reg.	Linear Reg.	1 linear layer	16,512	—
California Housing	Reg.	MLP	3 hidden blocks [128, 128, 128]	16,512	—
BloodMNIST	Classif.	DINO	DINOv2 ViT-S/14 (frozen + linear head)	8,000	8
CIFAR-10	Classif.	CNN	3 conv blocks,	50,000	10
CIFAR-100	Classif.	ResNet-20	3 stages, dropout 0.3	50,000	100
SST-2	Classif.	BERT	BERT-tiny (L=2, H=128),	67,349	2
SST-2	Classif.	BERT	BERT-base (frozen + linear head)	67,349	2

Table 3: Training hyperparameters. Loss is quadratic for regression and cross-entropy for classification.

Dataset	Model	Epochs	Batch	LR	Optimizer	Weight decay
UCI Energy	MLP	300	32	$10^{-3}$	Adam	$10^{-3}$
California Housing	Linear Reg.	200	256	$10^{-2}$	Adam	$10^{-3}$
California Housing	MLP	200	256	$10^{-3}$	Adam	$5 \cdot 10^{-4}$
BloodMNIST	DINO (linear)	100	512	$10^{-2}$	SGD ( $\mu=0.9$ )	$10^{-6}$
CIFAR-10	CNN	25	256	$10^{-3}$	AdamW	$5 \cdot 10^{-4}$
CIFAR-100	ResNet-20	50	256	$10^{-3}$	SGD ( $\mu=0.9$ )	$5 \cdot 10^{-4}$
SST-2	BERT (full FT)	10	32	$10^{-4}$	AdamW	$10^{-2}$
SST-2	BERT (linear)	10	32	$10^{-3}$	AdamW	$10^{-2}$

### C.2 Time and Compute Resources

All experiments were run using V100 (32 GB) GPU. The values presented in Table 4 are the wall-clock times reported using dedicated packages. They split into four phases: (i) training the reference ensemble, (ii) training the target models, (iii) running the LiRA, RMIA and Shokri attacks plus the per-point statistics, and (iv) computing the leverage-score / influence / Newton surrogates on each target. We report the total time spent in each phase, as well as the total time for the entire benchmark.

To evaluate cost-effectiveness, surrogate performance is reported as the time required to compute scores for a single target, allowing a direct comparison with the training of the 200 reference models. While actual implementation involves computing scores across all targets, resulting in a total runtime approximately 16 times the per-target figure, the single-target metric highlights the efficiency gains. For example, using the DiNO linear model, computing

Table 4: Compute budget for our experimental setting. Values are observed run-times in GPU-hours. *Surrogates* aggregates the GPU time spent computing the influence / Newton scores surrogates over all targets.

Dataset / Model	Training		Attacks+Stats	Surrogates	IF (full network)	Total	
	per-model	200 refs	16 targets	200 refs	per-target	per-target	GPU-h
UCI Energy / MLP	30 s	1.7 h	8 min	30 s	3 s	–	1.7 h
California / Linear reg.	1 min	3.3 h	0.3 h	7 min	10 s	–	3.6 h
California / MLP	1 min	3.3 h	0.3 h	7 min	10 s	20 min	8.9 h
BloodMNIST / DINO (linear)	15 min	60.0 h	4.0 h	5 min	15 s	–	64.0 h
CIFAR-10 / CNN	4 min	13.0 h	1.0 h	20 min	30 s	2.2 h	49.2 h
CIFAR-100 / ResNet-20	13 min	44.4 h	3.5 h	45 min	1 min	–	48.5 h
SST-2 / BERT-tiny (full FT)	6 min	20 h	1.6 h	17 min	45 s	–	20.6 h
SST-2 / BERT-base (linear)	19 min	64.6 h	5.0 h	18 min	3 min	–	70 h
<b>Total</b>							<b>266 GPU-h</b>

surrogates for one target takes only 15 seconds; this represents a  $50,000\times$  speedup compared to the 60 hours required to train all the reference (shadow) models.

The training phase dominates the total cost. Once all models are trained, surrogates and attacks reuse the same models.

## D Additional Experimental Results

Detailed results for the LiRA ASR top- $k\%$  recall are reported in Table 5. We observe that the Newton and Influence surrogates outperform the loss surrogate across most datasets and architectures. Although the Spearman correlation is often higher for our surrogates, the absolute values remain quite low (except for the CIFAR datasets).

This suggests that the ranking of samples by our surrogates is not perfectly aligned with the ranking by the LiRA score, mostly for the points that are in the middle of the distribution. This is not surprising as the LiRA ASR score is very noisy in this part of the distribution. This intuition is confirmed by Figure 7: points in the middle of the distribution are scattered, whereas in the tails the ranking induced by the surrogates is much more consistent with the LiRA score.

### D.1 Comparison with full-network Influence functions

To evaluate the impact of the last-layer approximation, we computed full-network influence functions for CIFAR10 (CNN) and California Housing (MLP). These estimates were calculated using inverse Hessian-vector products [Pearlmutter, 1994] via the Conjugate Gradient (CG) algorithm [Hestenes and Stiefel, 1952]. We ensured CG convergence by setting a tolerance of  $10^{-2}$  and applying a notably high damping value of 10; while strictly necessary for the algorithm to converge in our case, such heavy damping inherently alters the resulting influence estimates.

As presented in Table 4, the computational overhead for the full-network approach is substantial: for CIFAR10, processing a single model took more than 2 hours, compared to only 30 seconds for the last-layer surrogate. Despite this significantly higher cost, the full-network influence function performed worse in identifying vulnerable samples. This suggests that the last-layer approximation not only offers a massive gain in efficiency but may also act as a useful regularizer by focusing on the most discriminative features. Furthermore, as noted by Basu et al. [2021], this underperformance may come from the inherent fragility and poor scaling of influence functions when applied to the non-convex landscapes of deep networks.

Figure 3 illustrates the top- $k\%$  recall with the additional full network influence function

surrogate  $\nabla \ell_i^\top H_\theta^{-1} \nabla \ell_i$ . The values are reported in the CIFAR-10 and California Housing (MLP) cells in Table 5.

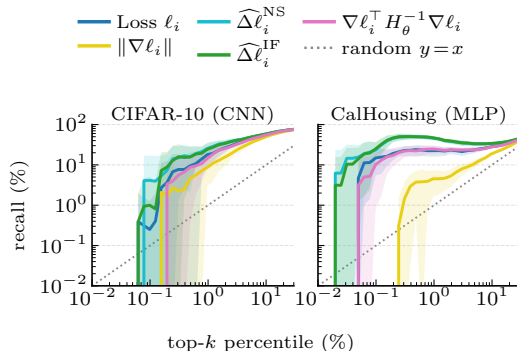


Figure 3: Recall of the top- $k$ % **LiRA**'s attack most vulnerable samples (ranked by the Average Success Rate) when keeping the top- $k$ % for each of the classical surrogates as well as the full Influence Function surrogate  $\nabla \ell_i^\top H_\theta^{-1} \nabla \ell_i$ . Axes are log-log; the dotted diagonal  $y = x$  is the random baseline. Solid lines are means over 16 target models with  $\pm 1$  std bands;

## D.2 Top- $k$ recall and Spearman correlation for LiRA attack

We report full results for the LiRA MIA in Table 5. Notably, we report the Spearman rank correlation between the surrogate scores and the per-point ASR for reference, but we do not find a strong correlation. We attribute this to the fact that points near the center of the vulnerability distribution yield an Attack Success Rate (ASR) close to 0.5, offering little informative value. In contrast, top- $k$  recall effectively isolates the highly vulnerable points, which are the primary focus for practical security auditing and defense.

For classification models we also report the self-entropy defined as  $H_i = -\sum_{k=1}^m \hat{p}_{i,k} \log \hat{p}_{i,k}$ , where  $\hat{p}_{i,k}$  is the model's predicted probability of class  $k$  on input  $x_i$ . Self-entropy is a standard confidence-based MIA baseline [Salem et al., 2018, Song and Mittal, 2021]: training samples typically receive more peaked predictions and hence lower entropy than non-members.

## D.3 Top- $k$ recall and Spearman correlation for RMIA attack and Classifier Shokri's attack

We provide the top- $k$  recall curves for RMIA and Shokri's attack in Figure 4 and Figure 5 respectively.

## D.4 Additional visualizations

We provide additional visualizations of the samples with the highest and lowest influence scores and Newton scores for the BloodMNIST, CIFAR-10 and CIFAR-100 datasets in Figure 6. We also provide the top-10 highest and lowest influence scores and Newton scores for the BERT model trained on the SST-2 dataset with linear probing in Table 6. The joint distribution of local loss  $\ell_i$  and influence score for every training sample of a single target model, colored by per-sample LiRA ASR, is presented in Figure 7.

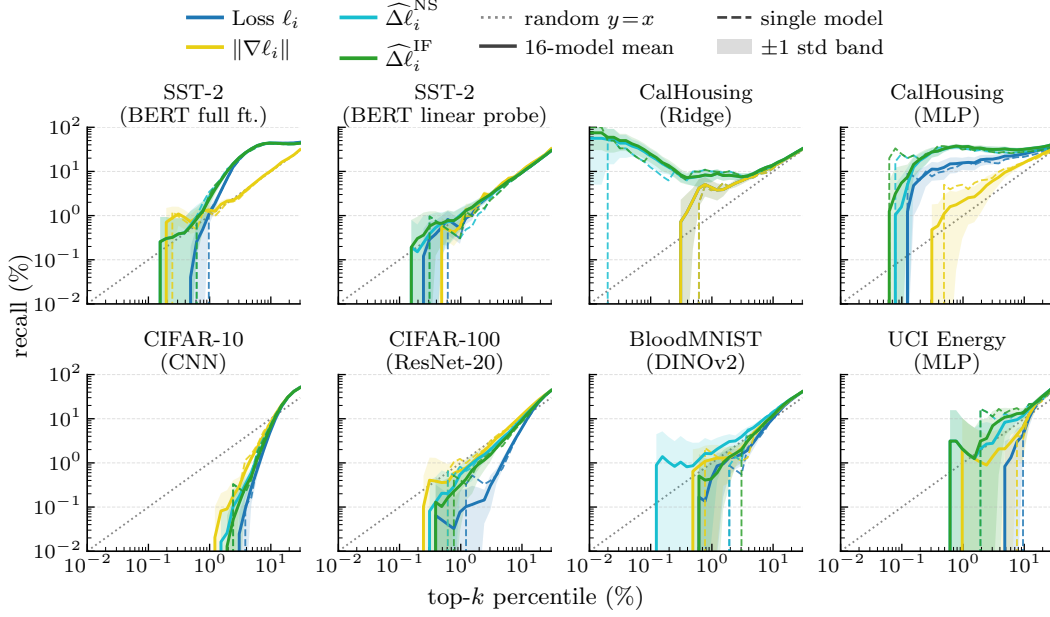


Figure 4: Recall of the top- $k\%$  **RMIA**'s attack most vulnerable samples (ranked by the Average Success Rate) when keeping the top- $k\%$  for each of the four surrogate: the loss  $\ell_i$ , the gradient norm  $\|\nabla\ell_i\|$ , the influence estimate  $\widehat{\Delta\ell}_i^{\text{IF}}$ , and the Newton estimate  $\widehat{\Delta\ell}_i^{\text{NS}}$ . Axes are log-log; the dotted diagonal  $y = x$  is the random baseline. Solid lines are means over 16 target models with  $\pm 1$  std bands; dashed-lines show a single representative model.

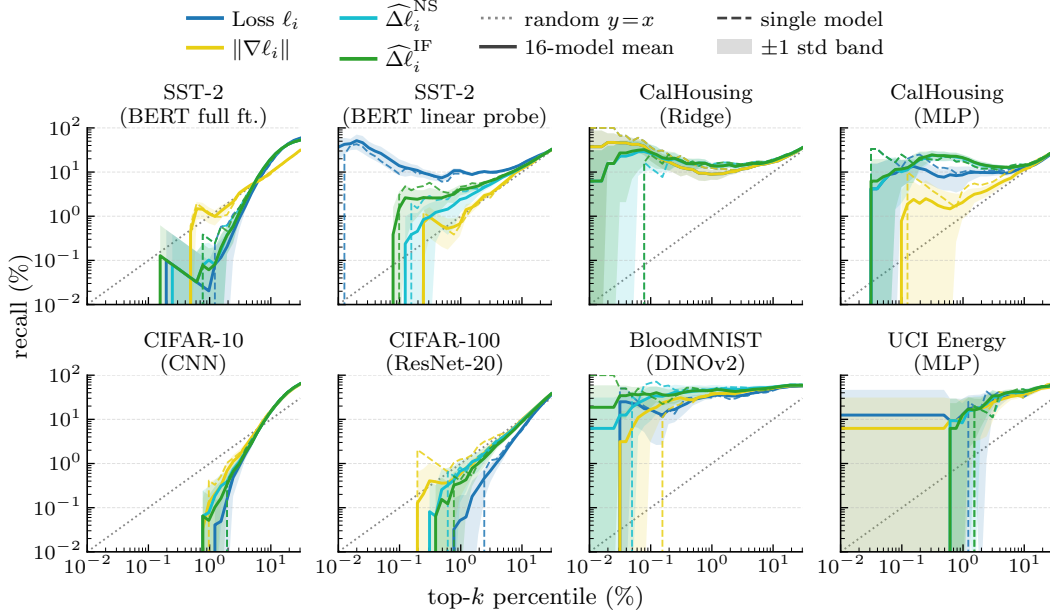


Figure 5: Recall of the top- $k\%$  **Shokri**'s attack most vulnerable samples (ranked by the Average Success Rate) when keeping the top- $k\%$  for each of the four surrogate: the loss  $\ell_i$ , the gradient norm  $\|\nabla\ell_i\|$ , the influence estimate  $\widehat{\Delta\ell}_i^{\text{IF}}$ , and the Newton estimate  $\widehat{\Delta\ell}_i^{\text{NS}}$ . Axes are log-log; the dotted diagonal  $y = x$  is the random baseline. Solid lines are means over 16 target models with  $\pm 1$  std bands; dashed-lines show a single representative model.

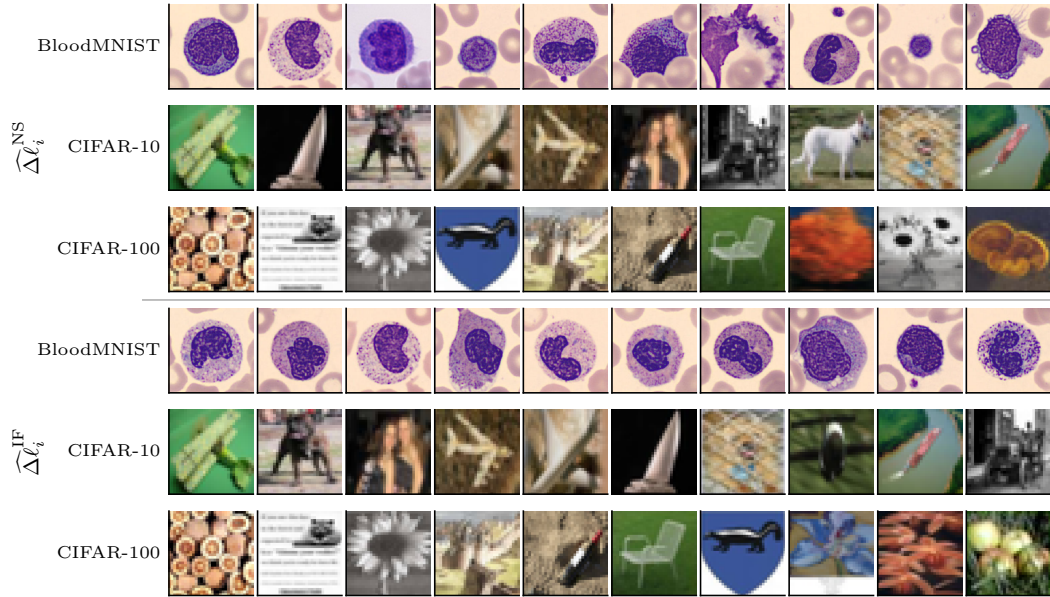


Figure 6: Visualization of the 10 images with the highest influence and Newton scores for BloodMNIST (top), CIFAR-10 (middle) and CIFAR-100 (bottom).

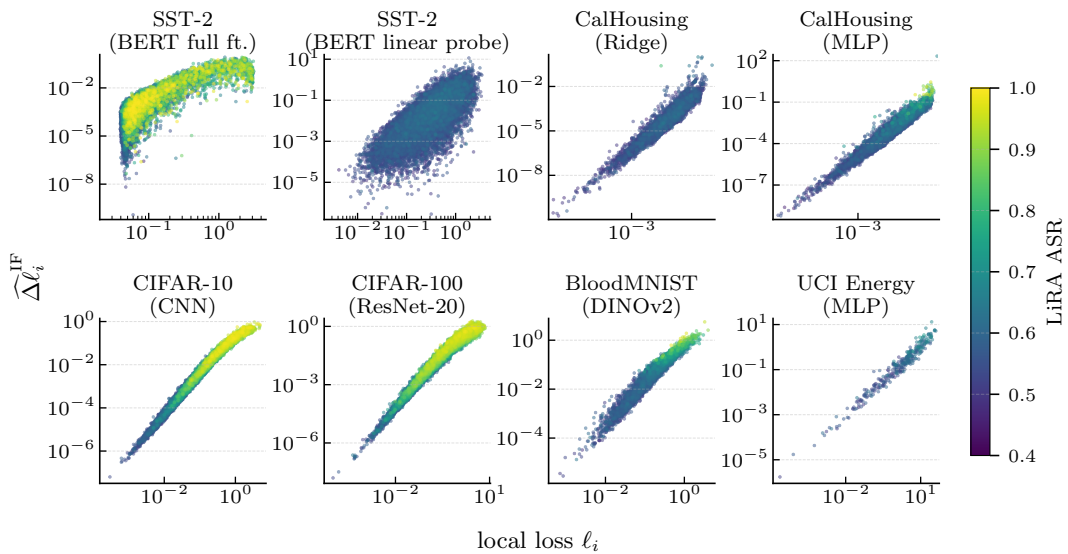


Figure 7: Joint distribution of local loss  $\ell_i$  and influence for every training sample of a single target model, coloured by per-sample LiRA ASR, log-log axes.

Table 5: LiRA membership-inference attack: top- $k$  recall (%) and Spearman rank correlation. Best results per dataset are in **bold**. Contrast with Table 1, the recall values here are when seeking the top- $k$  samples with the highest surrogates scores, by keeping the top- $k$  samples with the highest surrogate scores and checking how many of them are in the top- $k$  samples with the highest LiRA ASR score.

Dataset	Surrogate	Recall (%)			Spearman $\rho$
		@0.1%	@1%	@5%	
SST2 (BERT, full ft.)	Loss $\ell_i$	0.00 $\pm$ 0.00	5.44 $\pm$ 1.36	30.83 $\pm$ 1.11	<b>0.474 <math>\pm</math> 0.022</b>
	$\ \nabla\ell_i\ $	0.00 $\pm$ 0.00	0.57 $\pm$ 0.18	4.64 $\pm$ 0.33	–
	Self-entropy	0.02 $\pm$ 0.06	6.34 $\pm$ 1.16	28.52 $\pm$ 1.10	0.470 $\pm$ 0.022
	$\widehat{\Delta\ell}_i^{\text{NS}}$	1.02 $\pm$ 1.47	<b>7.05 <math>\pm</math> 1.23</b>	<b>31.30 <math>\pm</math> 1.44</b>	0.389 $\pm$ 0.036
	$\widehat{\Delta\ell}_i^{\text{IF}}$	<b>1.22 <math>\pm</math> 1.54</b>	6.88 $\pm$ 1.30	31.28 $\pm$ 1.44	0.389 $\pm$ 0.036
SST2 (BERT, linear probe)	Loss $\ell_i$	0.05 $\pm$ 0.08	<b>2.30 <math>\pm</math> 0.64</b>	<b>7.94 <math>\pm</math> 0.50</b>	<b>0.045 <math>\pm</math> 0.005</b>
	$\ \nabla\ell_i\ $	0.00 $\pm$ 0.00	1.56 $\pm$ 0.70	6.64 $\pm$ 0.65	–
	Self-entropy	<b>0.60 <math>\pm</math> 1.26</b>	1.07 $\pm$ 0.46	5.60 $\pm$ 0.34	0.026 $\pm$ 0.005
	$\widehat{\Delta\ell}_i^{\text{NS}}$	0.00 $\pm$ 0.00	1.80 $\pm$ 0.87	6.88 $\pm$ 0.57	0.037 $\pm$ 0.005
	$\widehat{\Delta\ell}_i^{\text{IF}}$	0.30 $\pm$ 0.94	2.27 $\pm$ 0.70	7.01 $\pm$ 0.43	0.038 $\pm$ 0.005
CalHousing (ridge)	Loss $\ell_i$	6.33 $\pm$ 7.74	3.16 $\pm$ 1.81	8.65 $\pm$ 1.05	0.033 $\pm$ 0.006
	$\ \nabla\ell_i\ $	6.33 $\pm$ 7.74	3.16 $\pm$ 1.81	8.65 $\pm$ 1.05	0.033 $\pm$ 0.006
	$\widehat{\Delta\ell}_i^{\text{NS}}$	36.44 $\pm$ 15.34	<b>7.54 <math>\pm</math> 2.50</b>	9.30 $\pm$ 1.23	0.050 $\pm$ 0.007
	$\widehat{\Delta\ell}_i^{\text{IF}}$	<b>38.02 <math>\pm</math> 14.64</b>	<b>7.54 <math>\pm</math> 2.50</b>	<b>9.30 <math>\pm</math> 1.24</b>	<b>0.050 <math>\pm</math> 0.007</b>
	Loss $\ell_i$	14.90 $\pm$ 9.25	22.59 $\pm$ 6.49	23.58 $\pm$ 4.03	0.276 $\pm$ 0.028
CalHousing (MLP)	$\ \nabla\ell_i\ $	0.00 $\pm$ 0.00	4.53 $\pm$ 2.83	10.81 $\pm$ 2.26	0.198 $\pm$ 0.019
	$\widehat{\Delta\ell}_i^{\text{NS}}$	23.95 $\pm$ 11.89	45.84 $\pm$ 5.54	33.22 $\pm$ 3.96	0.297 $\pm$ 0.027
	$\widehat{\Delta\ell}_i^{\text{IF}}$	<b>25.49 <math>\pm</math> 11.97</b>	<b>46.46 <math>\pm</math> 4.79</b>	<b>33.46 <math>\pm</math> 3.88</b>	<b>0.297 <math>\pm</math> 0.027</b>
	$\nabla\ell_i^\top H_\theta^{-1} \nabla\ell_i$	–	24.57 $\pm$ 5.55	23.72 $\pm$ 2.85	0.266 $\pm$ 0.025
	Loss $\ell_i$	4.02 $\pm$ 3.23	17.30 $\pm$ 2.10	42.98 $\pm$ 1.17	0.813 $\pm$ 0.004
CIFAR-10 (CNN)	$\ \nabla\ell_i\ $	0.01 $\pm$ 0.05	8.40 $\pm$ 1.65	33.52 $\pm$ 1.28	0.811 $\pm$ 0.003
	Self-entropy	0.78 $\pm$ 1.57	10.36 $\pm$ 1.33	38.70 $\pm$ 1.35	0.808 $\pm$ 0.004
	$\widehat{\Delta\ell}_i^{\text{NS}}$	<b>15.28 <math>\pm</math> 6.95</b>	<b>25.59 <math>\pm</math> 1.77</b>	<b>48.14 <math>\pm</math> 1.27</b>	0.814 $\pm$ 0.003
	$\widehat{\Delta\ell}_i^{\text{IF}}$	14.07 $\pm$ 7.06	24.48 $\pm$ 1.99	47.76 $\pm$ 1.31	<b>0.814 <math>\pm</math> 0.003</b>
	$\nabla\ell_i^\top H_\theta^{-1} \nabla\ell_i$	–	24.57 $\pm$ 5.55	23.72 $\pm$ 2.85	0.266 $\pm$ 0.025
CIFAR-100 (ResNet-20)	Loss $\ell_i$	2.26 $\pm$ 2.86	7.40 $\pm$ 1.80	20.53 $\pm$ 0.72	0.658 $\pm$ 0.007
	$\ \nabla\ell_i\ $	0.51 $\pm$ 1.39	2.68 $\pm$ 0.69	13.94 $\pm$ 0.93	0.659 $\pm$ 0.005
	Self-entropy	0.25 $\pm$ 0.99	3.84 $\pm$ 1.15	19.75 $\pm$ 1.11	0.686 $\pm$ 0.007
	$\widehat{\Delta\ell}_i^{\text{NS}}$	4.84 $\pm$ 4.60	<b>13.51 <math>\pm</math> 2.82</b>	<b>28.64 <math>\pm</math> 3.15</b>	<b>0.690 <math>\pm</math> 0.024</b>
	$\widehat{\Delta\ell}_i^{\text{IF}}$	<b>5.77 <math>\pm</math> 3.82</b>	13.08 $\pm$ 2.66	28.24 $\pm$ 2.80	0.689 $\pm$ 0.022
BloodMNIST (DINOv2)	Loss $\ell_i$	10.55 $\pm$ 10.08	33.22 $\pm$ 3.72	59.06 $\pm$ 2.19	0.600 $\pm$ 0.005
	$\ \nabla\ell_i\ $	10.91 $\pm$ 14.54	39.95 $\pm$ 4.54	62.34 $\pm$ 2.07	0.604 $\pm$ 0.005
	Self-entropy	0.00 $\pm$ 0.00	14.67 $\pm$ 3.72	44.45 $\pm$ 2.05	0.586 $\pm$ 0.005
	$\widehat{\Delta\ell}_i^{\text{NS}}$	<b>34.70 <math>\pm</math> 26.66</b>	<b>52.68 <math>\pm</math> 15.24</b>	67.00 $\pm$ 10.01	0.604 $\pm$ 0.031
	$\widehat{\Delta\ell}_i^{\text{IF}}$	27.24 $\pm$ 17.77	47.27 $\pm$ 7.87	<b>67.09 <math>\pm</math> 6.55</b>	<b>0.608 <math>\pm</math> 0.024</b>
UCI Energy (tab. MLP)	Loss $\ell_i$	0.00 $\pm$ 0.00	2.01 $\pm$ 8.06	20.74 $\pm$ 4.87	0.528 $\pm$ 0.040
	$\ \nabla\ell_i\ $	0.00 $\pm$ 0.00	6.25 $\pm$ 12.92	26.83 $\pm$ 9.21	0.507 $\pm$ 0.036
	$\widehat{\Delta\ell}_i^{\text{NS}}$	0.00 $\pm$ 0.00	10.90 $\pm$ 19.74	28.25 $\pm$ 7.50	<b>0.541 <math>\pm</math> 0.032</b>
	$\widehat{\Delta\ell}_i^{\text{IF}}$	<b>6.25 <math>\pm</math> 25.00</b>	<b>14.72 <math>\pm</math> 23.99</b>	<b>30.32 <math>\pm</math> 7.89</b>	0.540 $\pm$ 0.032

Table 6: Top-10 highest-|leverage| training sentences for BERT (linear probe) on SST2, ranked by Newton (left) and Influence (right) surrogates.

Rank	$\widehat{\Delta\ell}_i^{\text{NS}}$	$\widehat{\Delta\ell}_i^{\text{IF}}$
1	to appearing in this junk that 's tv sitcom material at best	is never quite able to overcome the cultural moat surrounding its l...
2	the filmmakers wisely decided to let crocodile hunter steve irwin d...	spider-man
3	the kind that pretends to be passionate and truthful but is really ...	nicks refuses to let slackers be seen as just another teen movie , ...
4	a supernatural mystery that does n't know whether it wants to be a ...	recycle images and characters that were already tired 10 years ago
5	less the cheap thriller you 'd expect than it is a fairly revealing...	report that the children of varying ages in my audience never cough...
6	played-out	breach gaps in their relationships with their fathers
7	of a callow rich boy who is forced to choose between his beautiful ...	it 's painful to watch witherspoon 's talents wasting away inside u...
8	that collect a bunch of people who are enthusiastic about something...	its drastic iconography
9	: the widowmaker is derivative , overlong , and bombastic – yet su...	of a callow rich boy who is forced to choose between his beautiful ...
10	ride around a pretty tattered old carousel .	never does " lilo & stitch " reach the emotion or timelessness of...